Systematic perturbation theory for dynamical coarse-graining

Gernot Schaller,* Philipp Zedler, and Tobias Brandes
Institut für Theoretische Physik, Technische Universität Berlin, Hardenbergstraße 36, 10623 Berlin, Germany
(Received 15 December 2008; published 20 March 2009)

We demonstrate how the dynamical coarse-graining approach can be systematically extended to higher orders in the coupling between system and reservoir. Up to second order in the coupling constant, we explicitly show that dynamical coarse-graining unconditionally preserves positivity of the density matrix—even for bath density matrices that are not in equilibrium and also for time-dependent system Hamiltonians. By construction, the approach correctly captures the short-time dynamics; i.e., it is suitable for analyzing non-Markovian effects. We compare the dynamics with the exact solution for highly non-Markovian systems and find a remarkable quality of the coarse-graining approach. The extension to higher orders is straightforward but rather tedious. The approach is especially useful for bath correlation functions of simple structure and for small system dimensions.

DOI: 10.1103/PhysRevA.79.032110 PACS number(s): 03.65.Yz

I. INTRODUCTION

The insight that quantum computers may solve certain problems such as number factoring [1] and database search [2] more efficiently than conventional computers has given rise to the field of quantum information (for an overview see, e.g., [3]). The conventional paradigm of quantum computation relies on unitary operations that act on low-dimensional subspaces of the 2^n-dimensional Hilbert space of n two-level systems—conventionally called qubits. Unfortunately, the dynamics of open quantum systems is not always unitary [4], such that the impact of decoherence has to be taken into account. This problem also affects alternative schemes such as one-way [5,6], holonomic [7], or adiabatic [8] quantum computation. Beyond this, the study of decoherence effects is of general interest in the control of quantum systems.

Often, the dynamics of open quantum systems is analyzed within the Born-Markov approximation scheme [4,9]. An important criticism raised against this scheme is that it does not generally preserve positivity of the reduced density matrix [10–13], which however is necessary for its probability interpretation [14]. In addition, the Born-Markov master equation cannot be expected to yield good results for short times, which may in the context of quantum computation, for example, lead to false error estimates on required gate operation times, etc. [15,16].

A possible resolution for the latter problem is to study non-Markovian master equations (that explicitly depend on the density matrix at all previous times via a memory kernel). However, except for some special cases [17], non-Markovian master equations are also not guaranteed to preserve positivity, and corresponding counterexamples can be easily constructed [18]. Technically, master equations with memory can, for example, be solved efficiently when the bath correlation functions can be approximated by a few decaying exponentials [19]. In the general case, they are however difficult if not impossible to solve analytically. This difficulty transfers to the numerical solution as well. In order to evolve the density matrix at time t, one would generally have to evaluate the solution at all previous times $t' < t$, which corresponds to significant computational and storage efforts.

It is therefore interesting to investigate alternatives such as the dynamical coarse-graining (DCG) approach. Recently, it been analyzed up to second order in the system-reservoir coupling constant (Born approximation) [20]. Instead of solving a single quantum master equation, the coarse-graining approach defines a continuous set of master equations,

$$\dot{\boldsymbol{\rho}}_{\mathrm{S}}^{\tau} = \mathcal{L}^{\tau} \boldsymbol{\rho}_{\mathrm{S}}^{\tau}(t), \tag{1}$$

parametrized by the coarse-graining time τ and then interpolates through the set of solutions at $t = \tau$,

$$\overline{\boldsymbol{\rho}_{\mathrm{S}}}(t) = e^{\mathcal{L}^{t} \cdot t} \boldsymbol{\rho}_{\mathrm{S}}^{0}. \tag{2}$$

Since the Liouville superoperators $\mathcal{L}^{\tau}$ are of Lindblad form [21] for all $\tau > 0$, the second-order dynamical coarse-graining (DCG2) approach preserves positivity of the density matrix at all times [20]. Note that in the general case, the above solution cannot be obtained by solving a single Lindblad form master equation merely equipped with time-dependent coefficients and should therefore be regarded as truly non-Markovian [22]. The conventional Born-Markov secular limit is obtained by the limit $\tau \to \infty$, i.e., $\dot{\boldsymbol{\rho}}_{\mathrm{S}}^{\mathrm{BMS}} = \mathcal{L}^{\infty} \boldsymbol{\rho}_{\mathrm{S}}^{\mathrm{BMS}}$, whereas in the short-time limit, the exact full solution is approximated. In addition, it was found for some simple examples considered in [20] that in the weak-coupling limit, the method approximated the results of the non-Markovian master equation for all times remarkably well.

The purpose of the present paper is twofold. By introducing coarse-graining in the interaction picture in Sec. II, we rigorously demonstrate that the method will approximate the exact solution for short times by construction; i.e., the method is suitable for studying non-Markovian effects. By including higher orders in the coupling constant, the agreement between coarse-graining and exact solution can be further improved. In addition, we show that up to second order

*schaller@itp.physik.tu-berlin.de

the method unconditionally preserves positivity of the density matrix, i.e., even for bath density matrices that do not commute with the bath Hamiltonian and/or for time-dependent system Hamiltonians. We will give several examples for finite-size "baths" (Secs. III A and III B) and the spin-boson model in Sec. III C, and we also consider fermionic models with transport in Sec. III D.

II. DCG IN THE INTERACTION PICTURE

A. Preliminaries

We consider systems where the time-independent Hamiltonian can be divided into three parts,

$$H = H_S + H_{SB} + H_B, \tag{3}$$

where H_S denotes the system Hamiltonian, H_B denotes the bath (reservoir) Hamiltonian (with $[H_S, H_B]=0$), and

$$H_{SB} = \lambda \sum_\alpha A_\alpha \otimes B_\alpha \tag{4}$$

couples the two by system (A_α) and bath (B_α) operators. Note that thereby one has by construction $[A_\alpha, B_\beta]=0$ (see Sec. III D for obtaining such a decomposition for fermionic systems with transport).

Note that Hermiticity of $H_{SB}=H_{SB}^\dagger$ imposes some constraints on the coupling operators. For example, it is always possible to perform a suitable redefinition of operators by splitting into Hermitian and anti-Hermitian parts ($A_\alpha = A_\alpha^H + A_\alpha^A$ and $B_\alpha = B_\alpha^H + B_\alpha^A$, for system and bath operators, respectively) to obtain $H_{SB}=\frac{1}{2}(H_{SB}+H_{SB}^\dagger) = \sum_\alpha [A_\alpha^H B_\alpha^H - i A_\alpha^A i B_\alpha^A]$, such that one can always assume Hermitian coupling operators $\tilde{A}_\alpha = \tilde{A}_\alpha^\dagger$ as well as $\tilde{B}_\alpha = \tilde{B}_\alpha^\dagger$ [4]. For the sake of convenience however, we will not assume this form here unless stated otherwise. We will use $\lambda < 1$ as a perturbation parameter (α-dependent coupling constants can be absorbed in the operator definitions).

In the interaction picture (where we will denote all operators by bold symbols)

$$\boldsymbol{\rho}(t) = e^{+i(H_S+H_B)t} \rho(t) e^{-i(H_S+H_B)t},$$

$$\boldsymbol{A_\alpha}(t) = e^{+iH_S t} A_\alpha e^{-iH_S t},$$

$$\boldsymbol{B_\alpha}(t) = e^{+iH_B t} B_\alpha e^{-iH_B t}, \tag{5}$$

the von Neumann equation reads

$$\dot{\boldsymbol{\rho}} = -i[\boldsymbol{H_{SB}}(t), \boldsymbol{\rho}(t)], \tag{6}$$

which is formally solved by $\boldsymbol{\rho}(t) = \boldsymbol{U}(t)\rho_0 \boldsymbol{U}^\dagger(t)$.

B. Perturbative expansion

The time-evolution operator in the interaction picture is governed by $\dot{\boldsymbol{U}} = -i\boldsymbol{H_{SB}}(t)\boldsymbol{U}(t)$, which can be solved iteratively. We can define the truncated time-evolution operator in the interaction picture via

$$\boldsymbol{U_n}(t) = \sum_{k=0}^{n} (-i)^k \int_0^t \boldsymbol{H_{SB}}(t_1) \cdots \boldsymbol{H_{SB}}(t_k) \times \Theta(t_1 - t_2) \cdots \Theta(t_{k-1} - t_k) dt_1 \cdots dt_k, \tag{7}$$

where the time ordering is expressed by Heaviside step functions. The above operator is unitary up to order of λ^n (assuming that $\boldsymbol{H_{SB}} = O\{\lambda\}$), i.e., $\boldsymbol{U_n}(t)\boldsymbol{U_n}^\dagger(t) = \mathbf{1} + O\{\lambda^{n+1}\}$. Specifically, one has up to fourth order

$$\boldsymbol{U}_4(t) = \mathbf{1} - i\lambda \mathcal{V}_1(t) - \lambda^2 \mathcal{V}_2(t) + i\lambda^3 \mathcal{V}_3(t) + \lambda^4 \mathcal{V}_4(t), \tag{8}$$

where we can use Eq. (4) to find for the operators

$$\mathcal{V}_1(t) \equiv \sum_\alpha \int_0^t dt_1 \boldsymbol{A_\alpha}(t_1) \boldsymbol{B_\alpha}(t_1),$$

$$\mathcal{V}_2(t) \equiv \sum_{\alpha\beta} \int_0^t dt_1 dt_2 \Theta(t_1 - t_2) \boldsymbol{A_\alpha}(t_1) \boldsymbol{B_\alpha}(t_1) \boldsymbol{A_\beta}(t_2) \boldsymbol{B_\beta}(t_2),$$

$$\mathcal{V}_3(t) \equiv \sum_{\alpha\beta\gamma} \int_0^t dt_1 dt_2 dt_3 \Theta(t_1 - t_2)\Theta(t_2 - t_3) \times \boldsymbol{A_\alpha}(t_1)\boldsymbol{B_\alpha}(t_1)\boldsymbol{A_\beta}(t_2)\boldsymbol{B_\beta}(t_2)\boldsymbol{A_\gamma}(t_3)\boldsymbol{B_\gamma}(t_3),$$

$$\mathcal{V}_4(t) \equiv \sum_{\alpha\beta\gamma\delta} \int_0^t \Theta(t_1 - t_2)\Theta(t_2 - t_3)\Theta(t_3 - t_4) \times \boldsymbol{A_\alpha}(t_1)\boldsymbol{B_\alpha}(t_1)\boldsymbol{A_\beta}(t_2)\boldsymbol{B_\beta}(t_2) \times \boldsymbol{A_\gamma}(t_3)\boldsymbol{B_\gamma}(t_3)\boldsymbol{A_\delta}(t_4)\boldsymbol{B_\delta}(t_4) dt_1 dt_2 dt_3 dt_4. \tag{9}$$

Using these expressions in the formal solution of the density matrix and collecting all terms of the same order, we obtain

$$\begin{aligned}\boldsymbol{\rho}(t) = {}& \boldsymbol{\rho}_0 - i\lambda[-\boldsymbol{\rho}_0 \mathcal{V}_1^\dagger(t) + \mathcal{V}_1(t)\boldsymbol{\rho}_0] + \lambda^2[-\boldsymbol{\rho}_0 \mathcal{V}_2^\dagger(t) \\ &+ \mathcal{V}_1(t)\boldsymbol{\rho}_0 \mathcal{V}_1^\dagger(t) - \mathcal{V}_2(t)\boldsymbol{\rho}_0] - i\lambda^3[\boldsymbol{\rho}_0 \mathcal{V}_3^\dagger(t) - \mathcal{V}_1(t)\boldsymbol{\rho}_0 \mathcal{V}_2^\dagger(t) \\ &+ \mathcal{V}_2(t)\boldsymbol{\rho}_0 \mathcal{V}_1^\dagger(t) - \mathcal{V}_3(t)\boldsymbol{\rho}_0] + \lambda^4[\boldsymbol{\rho}_0 \mathcal{V}_4^\dagger(t) - \mathcal{V}_1(t)\boldsymbol{\rho}_0 \mathcal{V}_3^\dagger(t) \\ &+ \mathcal{V}_2(t)\boldsymbol{\rho}_0 \mathcal{V}_2^\dagger(t) - \mathcal{V}_3(t)\boldsymbol{\rho}_0 \mathcal{V}_1^\dagger(t) + \mathcal{V}_4(t)\boldsymbol{\rho}_0] + O\{\lambda^5\}.\end{aligned} \tag{10}$$

In order to obtain the reduced density matrix, we have to perform the trace over the bath degrees of freedom. We assume that at $t_0=0$ the density matrix factorizes such that we have $\boldsymbol{\rho}_S^0 = \mathrm{Tr}_B\{\boldsymbol{\rho}_0\}$. Then we can define $\boldsymbol{\rho_S}(t) = \mathrm{Tr}_B\{\boldsymbol{\rho}(t)\}$ and calculate the reduced density matrix at time t,

$$\begin{aligned}\boldsymbol{\rho_S}(t) = {}& \boldsymbol{\rho}_S^0 - i\lambda\, \mathrm{Tr}_B\{-\boldsymbol{\rho}_S^0 \rho_B^0 \mathcal{V}_1^\dagger + \mathcal{V}_1 \boldsymbol{\rho}_S^0 \rho_B^0\} \\ &+ \lambda^2\, \mathrm{Tr}_B\{-\boldsymbol{\rho}_S^0 \rho_B^0 \mathcal{V}_2^\dagger + \mathcal{V}_1 \boldsymbol{\rho}_S^0 \rho_B^0 \mathcal{V}_1^\dagger - \mathcal{V}_2 \boldsymbol{\rho}_S^0 \rho_B^0\} \\ &- i\lambda^3\, \mathrm{Tr}_B\{\boldsymbol{\rho}_S^0 \rho_B^0 \mathcal{V}_3^\dagger - \mathcal{V}_1 \boldsymbol{\rho}_S^0 \rho_B^0 \mathcal{V}_2^\dagger + \mathcal{V}_2 \boldsymbol{\rho}_S^0 \rho_B^0 \mathcal{V}_1^\dagger - \mathcal{V}_3 \boldsymbol{\rho}_S^0 \rho_B^0\} \\ &+ \lambda^4\, \mathrm{Tr}_B\{\boldsymbol{\rho}_S^0 \rho_B^0 \mathcal{V}_4^\dagger - \mathcal{V}_1 \boldsymbol{\rho}_S^0 \rho_B^0 \mathcal{V}_3^\dagger + \mathcal{V}_2 \boldsymbol{\rho}_S^0 \rho_B^0 \mathcal{V}_2^\dagger \\ &- \mathcal{V}_3 \boldsymbol{\rho}_S^0 \rho_B^0 \mathcal{V}_1^\dagger + \mathcal{V}_4 \boldsymbol{\rho}_S^0 \rho_B^0\} + O\{\lambda^5\} \\ \equiv {}& \boldsymbol{\rho}_S^0 + \lambda \boldsymbol{\mathcal{T}}^t_1 \boldsymbol{\rho}_S^0 + \lambda^2 \boldsymbol{\mathcal{T}}^t_2 \boldsymbol{\rho}_S^0 + \lambda^3 \boldsymbol{\mathcal{T}}^t_3 \boldsymbol{\rho}_S^0 + \lambda^4 \boldsymbol{\mathcal{T}}^t_4 \boldsymbol{\rho}_S^0 \\ &+ O\{\lambda^5\},\end{aligned} \tag{11}$$

where we can evaluate the right-hand side by using the reservoir correlation functions; see below.

C. Bath correlation functions

Since we do neither assume *a priori* that the coupling operators are Hermitian nor that $[H_B, \rho_B^0]=0$, it is necessary to generalize the correlation functions. Denoting the index of a Hermitian conjugate coupling operator with an overbar, we define for the first and second orders

$$C_\alpha(t_1) \equiv \mathrm{Tr}_B\{\mathbf{B}_\alpha(t_1)\rho_B^0\},$$

$$C_{\bar\alpha}(t_1) \equiv \mathrm{Tr}_B\{\mathbf{B}_\alpha^\dagger(t_1)\rho_B^0\},$$

$$C_{\alpha\beta}(t_1,t_2) \equiv \mathrm{Tr}_B\{\mathbf{B}_\alpha(t_1)\mathbf{B}_\beta(t_2)\rho_B^0\},$$

$$C_{\alpha\bar\beta}(t_1,t_2) \equiv \mathrm{Tr}_B\{\mathbf{B}_\alpha(t_1)\mathbf{B}_\beta^\dagger(t_2)\rho_B^0\}, \qquad (12)$$

and similarly for higher orders. In terms of these quantities, the right-hand side of Eq. (11) can be easily evaluated. Specifically, we obtain

$$\mathcal{T}_1^t\boldsymbol{\rho}_S^0 = -i\sum_\alpha \int_0^t dt_1[-C_{\bar\alpha}(t_1)\boldsymbol{\rho}_S^0\boldsymbol{A}_\alpha^\dagger(t_1) + C_\alpha(t_1)\boldsymbol{A}_\alpha(t_1)\boldsymbol{\rho}_S^0],$$

$$\mathcal{T}_2^t\boldsymbol{\rho}_S^0 = \sum_{\alpha\beta}\int_0^t dt_1dt_2[-C_{\bar\alpha\bar\beta}(t_1,t_2)\Theta(t_2-t_1)\boldsymbol{\rho}_S^0\boldsymbol{A}_\alpha^\dagger(t_1)\boldsymbol{A}_\beta^\dagger(t_2) + C_{\bar\alpha\beta}(t_1,t_2)\boldsymbol{A}_\beta(t_2)\boldsymbol{\rho}_S^0\boldsymbol{A}_\alpha^\dagger(t_1) - C_{\alpha\beta}(t_1,t_2)\Theta(t_1-t_2)\boldsymbol{A}_\alpha(t_1)\boldsymbol{A}_\beta(t_2)\boldsymbol{\rho}_S^0],$$

$$\begin{aligned}\mathcal{T}_3^t\boldsymbol{\rho}_S^0 = -i\sum_{\alpha\beta\gamma}\int_0^t dt_1dt_2dt_3[&+C_{\bar\alpha\bar\beta\bar\gamma}(t_1,t_2,t_3)\Theta(t_3-t_2)\Theta(t_2-t_1)\boldsymbol{\rho}_S^0\boldsymbol{A}_\alpha^\dagger(t_1)\boldsymbol{A}_\beta^\dagger(t_2)\boldsymbol{A}_\gamma^\dagger(t_3)\\ &- C_{\bar\alpha\bar\beta\gamma}(t_1,t_2,t_3)\Theta(t_2-t_1)\boldsymbol{A}_\gamma(t_3)\boldsymbol{\rho}_S^0\boldsymbol{A}_\alpha^\dagger(t_1)\boldsymbol{A}_\beta^\dagger(t_2) + C_{\bar\alpha\beta\gamma}(t_1,t_2,t_3)\Theta(t_2-t_3)\boldsymbol{A}_\beta(t_2)\boldsymbol{A}_\gamma(t_3)\boldsymbol{\rho}_S^0\boldsymbol{A}_\alpha^\dagger(t_1)\\ &- C_{\alpha\beta\gamma}(t_1,t_2,t_3)\Theta(t_1-t_2)\Theta(t_2-t_3)\boldsymbol{A}_\alpha(t_1)\boldsymbol{A}_\beta(t_2)\boldsymbol{A}_\gamma(t_3)\boldsymbol{\rho}_S^0],\end{aligned}$$

$$\begin{aligned}\mathcal{T}_4^t\boldsymbol{\rho}_S^0 = \sum_{\alpha\beta\gamma\delta}\int_0^t dt_1dt_2dt_3dt_4[&+C_{\bar\alpha\bar\beta\bar\gamma\bar\delta}(t_1,t_2,t_3,t_4)\Theta(t_4-t_3)\Theta(t_3-t_2)\Theta(t_2-t_1)\boldsymbol{\rho}_S^0\boldsymbol{A}_\alpha^\dagger(t_1)\boldsymbol{A}_\beta^\dagger(t_2)\boldsymbol{A}_\gamma^\dagger(t_3)\boldsymbol{A}_\delta^\dagger(t_4)\\ &- C_{\bar\alpha\bar\beta\bar\gamma\delta}(t_1,t_2,t_3,t_4)\Theta(t_3-t_2)\Theta(t_2-t_1)\boldsymbol{A}_\delta(t_4)\boldsymbol{\rho}_S^0\boldsymbol{A}_\alpha^\dagger(t_1)\boldsymbol{A}_\beta^\dagger(t_2)\boldsymbol{A}_\gamma^\dagger(t_3)\\ &+ C_{\bar\alpha\bar\beta\gamma\delta}(t_1,t_2,t_3,t_4)\Theta(t_3-t_4)\Theta(t_2-t_1)\boldsymbol{A}_\gamma(t_3)\boldsymbol{A}_\delta(t_4)\boldsymbol{\rho}_S^0\boldsymbol{A}_\alpha^\dagger(t_1)\boldsymbol{A}_\beta^\dagger(t_2)\\ &- C_{\bar\alpha\beta\gamma\delta}(t_1,t_2,t_3,t_4)\Theta(t_2-t_3)\Theta(t_3-t_4)\boldsymbol{A}_\beta(t_2)\boldsymbol{A}_\gamma(t_3)\boldsymbol{A}_\delta(t_4)\boldsymbol{\rho}_S^0\boldsymbol{A}_\alpha^\dagger(t_1)\\ &+ C_{\alpha\beta\gamma\delta}(t_1,t_2,t_3,t_4)\Theta(t_1-t_2)\Theta(t_2-t_3)\Theta(t_3-t_4)\boldsymbol{A}_\alpha(t_1)\boldsymbol{A}_\beta(t_2)\boldsymbol{A}_\gamma(t_3)\boldsymbol{A}_\delta(t_4)\boldsymbol{\rho}_S^0].\end{aligned} \qquad (13)$$

D. Defining the DCG Liouvillian

It is evident that one can carry on with the expansion of the time-evolution operator to arbitrary order in the coupling constant λ. This will evidently yield good results for small λ and small times, whereas we would like to have a master equation valid for small λ and also large times. In the original approach [20] it was shown as a supportive fact that for $t=\tau$ the DCG2 solution and approximation (11) were equivalent up to $O\{\lambda^2\}$. Here we will demand equivalence between the nth-order coarse-graining solution and Eq. (11) at $t=\tau$ to define our perturbation theory. Expanding the Liouvillian superoperator as $\mathcal{L}^\tau=\lambda\mathcal{L}_1^\tau+\lambda^2\mathcal{L}_2^\tau+\lambda^3\mathcal{L}_3^\tau+\lambda^4\mathcal{L}_4^\tau+O\{\lambda^5\}$, we obtain for the solution of $\dot{\boldsymbol{\rho}}_S^\tau(t)=\mathcal{L}^\tau\boldsymbol{\rho}_S^\tau(t)$ at time $t=\tau$ the following:

$$\begin{aligned}\boldsymbol{\rho}_S^\tau(\tau) = \Bigg\{&1+\lambda\tau\mathcal{L}_1^\tau+\lambda^2\left[\tau\mathcal{L}_2^\tau+\frac{\tau^2}{2}\mathcal{L}_1^\tau\mathcal{L}_1^\tau\right]\\ &+\lambda^3\left[\tau\mathcal{L}_3^\tau+\frac{\tau^2}{2}(\mathcal{L}_1^\tau\mathcal{L}_2^\tau+\mathcal{L}_2^\tau\mathcal{L}_1^\tau)+\frac{\tau^3}{6}\mathcal{L}_1^\tau\mathcal{L}_1^\tau\mathcal{L}_1^\tau\right]\\ &+\lambda^4\Bigg[\tau\mathcal{L}_4^\tau+\frac{\tau^2}{2}(\mathcal{L}_1^\tau\mathcal{L}_3^\tau+\mathcal{L}_2^\tau\mathcal{L}_2^\tau+\mathcal{L}_3^\tau\mathcal{L}_1^\tau)\\ &+\frac{\tau^3}{6}(\mathcal{L}_1^\tau\mathcal{L}_1^\tau\mathcal{L}_2^\tau+\mathcal{L}_1^\tau\mathcal{L}_2^\tau\mathcal{L}_1^\tau+\mathcal{L}_2^\tau\mathcal{L}_1^\tau\mathcal{L}_1^\tau)\\ &+\frac{\tau^4}{24}\mathcal{L}_1^\tau\mathcal{L}_1^\tau\mathcal{L}_1^\tau\mathcal{L}_1^\tau\Bigg]\Bigg\}\boldsymbol{\rho}_S^0+O\{\lambda^5\}\end{aligned} \qquad (14)$$

We can clearly match this with Eq. (11) evaluated at $t=\tau$ order by order to solve for

$$\mathcal{L}_1^\tau \boldsymbol{\rho}_S^0 = \frac{1}{\tau}\mathcal{T}_1^\tau \boldsymbol{\rho}_S^0,$$

$$\mathcal{L}_2^\tau \boldsymbol{\rho}_S^0 = \frac{1}{\tau}\left\{\mathcal{T}_2^\tau - \left[\frac{\tau^2}{2}\mathcal{L}_1^\tau\mathcal{L}_1^\tau\right]\right\}\boldsymbol{\rho}_S^0,$$

$$\mathcal{L}_3^\tau \boldsymbol{\rho}_S^0 = \frac{1}{\tau}\left\{\mathcal{T}_3^\tau - \left[\frac{\tau^2}{2}(\mathcal{L}_1^\tau\mathcal{L}_2^\tau + \mathcal{L}_2^\tau\mathcal{L}_1^\tau) + \frac{\tau^3}{6}\mathcal{L}_1^\tau\mathcal{L}_1^\tau\mathcal{L}_1^\tau\right]\right\}\boldsymbol{\rho}_S^0,$$

$$\mathcal{L}_4^\tau \boldsymbol{\rho}_S^0 = \frac{1}{\tau}\left\{\mathcal{T}_4^\tau - \left[\frac{\tau^2}{2}(\mathcal{L}_1^\tau\mathcal{L}_3^\tau + \mathcal{L}_2^\tau\mathcal{L}_2^\tau + \mathcal{L}_3^\tau\mathcal{L}_1^\tau) + \frac{\tau^3}{6}(\mathcal{L}_1^\tau\mathcal{L}_1^\tau\mathcal{L}_2^\tau + \mathcal{L}_1^\tau\mathcal{L}_2^\tau\mathcal{L}_1^\tau + \mathcal{L}_2^\tau\mathcal{L}_1^\tau\mathcal{L}_1^\tau) + \frac{\tau^4}{24}\mathcal{L}_1^\tau\mathcal{L}_1^\tau\mathcal{L}_1^\tau\mathcal{L}_1^\tau\right]\right\}\boldsymbol{\rho}_S^0, \tag{15}$$

where $\mathcal{T}_1^\tau, \mathcal{T}_2^\tau, \mathcal{T}_3^\tau, \mathcal{T}_4^\tau$ can be extracted from Eq. (13). Since these equations have to hold for all initial conditions $\boldsymbol{\rho}_S^0$, we can infer the matrix elements of each Liouvillian by comparing coefficients of the matrix elements of $\boldsymbol{\rho}_S^0$.

Equation (15) defines in combination with Eq. (13) our coarse-graining Liouvillian. Evidently, we automatically approximate the short-time dynamics of the true solution very well by construction with this scheme.

E. Unconditional positivity of DCG2

Here we will show that DCG2 always preserves positivity—regardless of whether the first-order correlation functions vanish or not. We do not even require that $[H_B, \rho_B^0]=0$. For simplicity we assume Hermitian coupling operators $A_\alpha = A_\alpha^\dagger$ and $B_\alpha = B_\alpha^\dagger$. Then, we obtain from Eq. (13)

$$\mathcal{T}_1^\tau \rho_S = -i\sum_\alpha \int_0^\tau dt_1 C_\alpha(t_1)[\boldsymbol{A}_\alpha(t_1)\rho_S - \rho_S \boldsymbol{A}_\alpha(t_1)],$$

$$\mathcal{T}_2^\tau \rho_S = \sum_{\alpha\beta}\int_0^\tau dt_1 dt_2 C_{\alpha\beta}(t_1,t_2)\left[\boldsymbol{A}_\beta(t_2)\rho_S\boldsymbol{A}_\alpha(t_1) - \frac{1}{2}\rho_S\boldsymbol{A}_\alpha(t_1)\boldsymbol{A}_\beta(t_2) - \frac{1}{2}\boldsymbol{A}_\alpha(t_1)\boldsymbol{A}_\beta(t_2)\rho_S\right] - i\sum_{\alpha\beta}\frac{1}{2i}\int_0^\tau C_{\alpha\beta}(t_1,t_2)\text{sgn}(t_1-t_2) \times [\boldsymbol{A}_\alpha(t_1)\boldsymbol{A}_\beta(t_2), \rho_S]dt_1 dt_2, \tag{16}$$

where we have used $\Theta(x)=\frac{1}{2}[1+\text{sgn}(x)]$ and $\text{sgn}(-x) = -\text{sgn}(x)$ in the last equation . From the first of the above equations, we obtain that the first-order Liouvillian just generates a unitary evolution

$$\mathcal{L}_1^\tau \rho_S = -i\left[\frac{1}{\tau}\sum_\alpha \int_0^\tau C_\alpha(t_1)\boldsymbol{A}_\alpha(t_1)dt_1, \rho_S\right] \equiv -i[\boldsymbol{H}_{\text{eff}}^{\tau,1}, \rho_S], \tag{17}$$

where Hermiticity of the Lamb-shift Hamiltonian follows directly from Hermiticity of the coupling operators (which also implies real-valued first-order correlation functions). In addition, we obtain from consecutive application

$$\frac{1}{2}\mathcal{T}_1^\tau\mathcal{T}_1^\tau \rho_S = \sum_{\alpha\beta}\int_0^\tau dt_1 dt_2 C_\alpha(t_1)C_\beta(t_2) \times \left[\boldsymbol{A}_\beta(t_2)\rho_S\boldsymbol{A}_\alpha(t_1) - \frac{1}{2}\{\rho_S, \boldsymbol{A}_\alpha(t_1)\boldsymbol{A}_\beta(t_2)\}\right]. \tag{18}$$

This defines the second-order Liouvillian as

$$\mathcal{L}_2^\tau \rho_S = -i\left[\frac{1}{2\tau i}\sum_{\alpha\beta}\int_0^\tau C_{\alpha\beta}(t_1,t_2)\text{sgn}(t_1-t_2) \times \boldsymbol{A}_\alpha(t_1)\boldsymbol{A}_\beta(t_2)dt_1 dt_2, \rho_S\right] + \frac{1}{\tau}\sum_{\alpha\beta}\int_0^\tau dt_1 dt_2 [C_{\alpha\beta}(t_1,t_2) - C_\alpha(t_1)C_\beta(t_2)] \times \left[\boldsymbol{A}_\beta(t_2)\rho_S\boldsymbol{A}_\alpha(t_1) - \frac{1}{2}\{\boldsymbol{A}_\alpha(t_1)\boldsymbol{A}_\beta(t_2), \rho_S\}\right]. \tag{19}$$

The first commutator term induces a unitary evolution where Hermiticity of the corresponding effective Hamiltonian follows directly from $C_{\beta\alpha}^*(t_2,t_1) = C_{\alpha\beta}(t_1,t_2)$. However, in contrast to the standard Born-Markov secular approximation [4], here we have in general $[\boldsymbol{H}_{\text{eff}}^{\tau,2}, H_S] \neq 0$. In order to see that the last expression corresponds to a Lindblad dissipator, we insert identities at suitable places $1 = \Sigma_a |a\rangle\langle a|$ to obtain

$$\mathcal{L}_2^\tau \rho_S = -i[\boldsymbol{H}_{\text{eff}}^{\tau,2}, \rho_S] + \sum_{ab,cd}\gamma_{ab,cd}^{\tau,2}\left[L_{ab}\rho_S L_{cd}^\dagger - \frac{1}{2}\{L_{cd}^\dagger L_{ab}, \rho_S\}\right],$$

$$\gamma_{ab,cd}^{\tau,2} = \frac{1}{\tau}\sum_{\alpha\beta}\int_0^\tau [C_{\alpha\beta}(t_1,t_2) - C_\alpha(t_1)C_\beta(t_2)]\langle a|\boldsymbol{A}_\beta(t_2)|b\rangle \times \langle c|\boldsymbol{A}_\alpha(t_1)|d\rangle^* dt_1 dt_2, \tag{20}$$

where we have abbreviated the operators $L_{ab} = |a\rangle\langle b|$. The dampening matrix elements can be most conveniently evaluated in the energy eigenbasis $H_S|a\rangle = E_a|a\rangle$.

However, independent of the basis choice it remains to be shown that the dampening matrix is positive semidefinite to get a Lindblad form. In order to see this, we calculate with Eq. (12)

$$\begin{aligned}
\sum_{abcd} x_{ab}^{*}\gamma_{ab,cd}^{\tau,2}x_{cd} &= \frac{1}{\tau}\sum_{abcd}\sum_{\alpha\beta} x_{ab}^{*}x_{cd}\int_0^{\tau} dt_1 dt_2 C_{\alpha\beta}(t_1,t_2)\langle a|\boldsymbol{A}_{\boldsymbol{\beta}}(t_2)|b\rangle\langle c|\boldsymbol{A}_{\boldsymbol{\alpha}}(t_1)|d\rangle^{*} \\
&\quad - \frac{1}{\tau}\sum_{abcd}\sum_{\alpha\beta} x_{ab}^{*}x_{cd}\int_0^{\tau} dt_1 dt_2 C_{\alpha}(t_1)C_{\beta}(t_2)\langle a|\boldsymbol{A}_{\boldsymbol{\beta}}(t_2)|b\rangle\langle c|\boldsymbol{A}_{\boldsymbol{\alpha}}(t_1)|d\rangle^{*} \\
&= \frac{1}{\tau}\mathrm{Tr_B}\left\{\left[\sum_{cd\alpha}\int_0^{\tau}\boldsymbol{B}_{\boldsymbol{\alpha}}(t_1)x_{cd}\langle c|\boldsymbol{A}_{\boldsymbol{\alpha}}(t_1)|d\rangle^{*}dt_1\right]\left[\sum_{ab\beta}\int_0^{\tau}\boldsymbol{B}_{\boldsymbol{\beta}}(t_2)x_{ab}^{*}\langle a|\boldsymbol{A}_{\boldsymbol{\beta}}(t_2)|b\rangle dt_2\right]\rho_{\mathrm{B}}^{0}\right\} \\
&\quad - \frac{1}{\tau}\mathrm{Tr_B}\left\{\sum_{cd\alpha}\int_0^{\tau}\boldsymbol{B}_{\boldsymbol{\alpha}}(t_1)x_{cd}\langle c|\boldsymbol{A}_{\boldsymbol{\alpha}}(t_1)|d\rangle^{*}dt_1\rho_{\mathrm{B}}^{0}\right\}\mathrm{Tr_B}\left\{\sum_{ab\beta}\int_0^{\tau}\boldsymbol{B}_{\boldsymbol{\beta}}(t_2)x_{ab}^{*}\langle a|\boldsymbol{A}_{\boldsymbol{\beta}}(t_2)|b\rangle dt_2\rho_{\mathrm{B}}^{0}\right\} \\
&\equiv \frac{1}{\tau}[\mathrm{Tr_B}\{K^{\dagger}(\tau)K(\tau)\rho_{\mathrm{B}}^{0}\} - \mathrm{Tr_B}\{K^{\dagger}(\tau)\rho_{\mathrm{B}}^{0}\}\mathrm{Tr_B}\{K(\tau)\rho_{\mathrm{B}}^{0}\}] \\
&= \frac{1}{\tau}[\mathrm{Tr_B}\{K^{\dagger}(\tau)K(\tau)\rho_{\mathrm{B}}^{0}\} - |\mathrm{Tr_B}\{K(\tau)\rho_{\mathrm{B}}^{0}\}|^2]. \qquad (21)
\end{aligned}$$

Whereas the first term in the last line appears positive, one might fear that positivity can be spoiled by the existence of the additional second term. However, we can bound the second term via the Cauchy-Schwarz trace inequality [23] $|\mathrm{Tr}\{AB\}|^2 \le \mathrm{Tr}\{A^{\dagger}A\}\mathrm{Tr}\{B^{\dagger}B\}$, with $A = K(\tau)\sqrt{\rho_{\mathrm{B}}^{0}}$ and $B = \sqrt{\rho_{\mathrm{B}}^{0}}$ (which exists as ρ_{B}^{0} is positive semidefinite),

$$\begin{aligned}
|\mathrm{Tr_B}\{K(\tau)\rho_{\mathrm{B}}^{0}\}|^2 &= |\mathrm{Tr_B}\{K(\tau)\sqrt{\rho_{\mathrm{B}}^{0}}\sqrt{\rho_{\mathrm{B}}^{0}}\}|^2 \\
&\le \mathrm{Tr_B}\{\sqrt{\rho_{\mathrm{B}}^{0}}K^{\dagger}(\tau)K(\tau)\sqrt{\rho_{\mathrm{B}}^{0}}\}\mathrm{Tr_B}\{\sqrt{\rho_{\mathrm{B}}^{0}}\sqrt{\rho_{\mathrm{B}}^{0}}\} \\
&= \mathrm{Tr_B}\{K^{\dagger}(\tau)K(\tau)\rho_{\mathrm{B}}^{0}\}. \qquad (22)
\end{aligned}$$

Remembering that $\mathrm{Tr_B}\{K^{\dagger}(\tau)K(\tau)\rho_{\mathrm{B}}^{0}\} \ge 0$ for any operator $K(\tau)$, we therefore obtain for $\tau \ge 0$

$$\sum_{abcd} x_{ab}^{*}\gamma_{ab,cd}^{\tau,2}x_{cd} \ge 0, \qquad (23)$$

i.e., we have generated a Lindblad form master equation. This result goes beyond Ref. [20] in several aspects. Not only is the case $C_{\alpha}(t_1) \neq 0$ considered but, in addition, we do not constrain ourselves to bath density matrices in thermal equilibrium; i.e., one also has positivity for $[\rho_{\mathrm{B}}^{0}, H_{\mathrm{B}}] \neq 0$. It is an interesting avenue of further research to compare DCG with other methods within the context of nonequilibrium environments [24]. Beyond that, all of the above arguments go through if the system Hamiltonian is time dependent. In this case, the coupling operators in the interaction picture have to obey $\dot{\boldsymbol{A}}_{\boldsymbol{\alpha}} = +i[H_{\mathrm{S}}(t), \boldsymbol{A}_{\boldsymbol{\alpha}}(t)]$, such that the challenge is then to calculate the matrix elements $\langle a|\boldsymbol{A}_{\boldsymbol{\alpha}}(t)|b\rangle$.

Under the assumptions $C_{\alpha}(t)=0$ (no first-order correlation functions) and $C_{\alpha\beta}(t_1,t_2) = C_{\alpha\beta}(t_1-t_2) \equiv \mathrm{Tr_B}\{\boldsymbol{B}_{\boldsymbol{\alpha}}(t_1-t_2)B_{\beta}\rho_{\mathrm{B}}^{0}\}$ (reservoir in thermal equilibrium), we can insert the Fourier transforms of $C_{\alpha\beta}(t_1-t_2)$ and $C_{\alpha\beta}(t_1-t_2)\mathrm{sgn}(t_1-t_2)$. If in addition the system Hamiltonian is time independent, we may calculate the time integrals analytically. Then, we can make use of the identity for discrete a and b (see, e.g., Appendix F of Ref. [20]),

$$\lim_{\tau\to\infty} \tau\,\mathrm{sinc}\left[\frac{(\omega+a)\tau}{2}\right]\mathrm{sinc}\left[\frac{(\omega+b)\tau}{2}\right] \sim 2\pi\delta_{ab}\delta(\omega+a), \qquad (24)$$

to calculate the large-time limit of the DCG2 approach. In complete analogy to Ref. [20], we obtain the Born-Markov secular approximation [4] in this limit.

Unfortunately, the unconditional preservation of positivity is not preserved by higher orders within DCG (although of course, in the weak-coupling limit the nice properties of DCG2 will dominate).

III. EXAMPLES

In the following, we will test the DCG approach with simple examples for which at least in special cases an analytical solution exists. For finite-size reservoirs the correlation functions are nondecaying and these systems are inherently non-Markovian (exhibiting, for example, recurrences); cf. the examples in Secs. III A and III B. For quasicontinuous reservoirs we will compare the performance of the DCG approach with the Born-Markov approximation; see Secs. III C and III D.

A. DCG2 for two spins

We consider a highly non-Markovian system (S) by using a very small reservoir (B), namely, just a single further spin,

$$H_{\mathrm{S}} = \omega\sigma_{\mathrm{S}}^{z}, \quad H_{\mathrm{B}} = \Omega\sigma_{\mathrm{B}}^{z},$$

$$H_{\mathrm{SB}} = \lambda\vec{\sigma}_{\mathrm{S}}\cdot\vec{\sigma}_{\mathrm{B}} = \lambda[\sigma_{\mathrm{S}}^{x}\otimes\sigma_{\mathrm{B}}^{x} + \sigma_{\mathrm{S}}^{y}\otimes\sigma_{\mathrm{B}}^{y} + \sigma_{\mathrm{S}}^{z}\otimes\sigma_{\mathrm{B}}^{z}], \qquad (25)$$

i.e., the index of the coupling operators runs from one to three. Note that all coupling operators are Hermitian, such that we may omit overbars and daggers in Eq. (13). We assume that the initial bath density matrix is diagonal in order to simplify all expressions,

$$\rho_B^0 = \begin{pmatrix} \rho_B^{00} & 0 \\ 0 & 1-\rho_B^{00} \end{pmatrix}.$$

The exact solution can be obtained by exponentiating the Hamiltonian and tracing out the bath spin (not shown). As in Sec. II E we decompose the Liouville operator into unitary and nonunitary contributions, where we have first- and second-order contributions in the unitary action of decoherence, $\boldsymbol{H}_{\text{eff}}^{\tau}=\boldsymbol{H}_{\text{eff}}^{\tau,1}+\boldsymbol{H}_{\text{eff}}^{\tau,2}$, and second-order contributions for the dissipative action $\gamma_{ab,cd}^{\tau}=\gamma_{ab,cd}^{\tau,2}$.

Transforming the coupling operators into the interaction picture, we obtain $\boldsymbol{B}_1(t)=\cos(2\Omega t)\sigma_B^x-\sin(2\Omega t)\sigma_B^y$, $\boldsymbol{A}_1(t)=\cos(2\omega t)\sigma_S^x-\sin(2\omega t)\sigma_S^y$, $\boldsymbol{B}_2(t)=\cos(2\Omega t)\sigma_B^y+\sin(2\Omega t)\sigma_B^x$, $\boldsymbol{A}_2(t)=\cos(2\omega t)\sigma_S^y+\sin(2\omega t)\sigma_S^x$, $\boldsymbol{B}_3(t)=\sigma_B^z$, and $\boldsymbol{A}_3(t)=\sigma_S^z$. From this, we obtain the time-independent first-order correlation functions

$$C_1(t)=0, \quad C_2(t)=0, \quad C_3(t)=2\rho_B^{00}-1, \tag{26}$$

which yield for the first-order Lamb shift Hamiltonian from Eq. (17) the following:

$$\boldsymbol{H}_{\text{eff}}^{\tau,1}=\lambda(2\rho_B^{00}-1)\sigma_S^z. \tag{27}$$

The nonvanishing second-order correlation functions equate to

$$C_{11}=\cos[2(t_1-t_2)\Omega]-i(1-2\rho_B^{00})\sin[2(t_1-t_2)\Omega],$$

$$C_{12}=-i(1-2\rho_B^{00})\cos[2(t_1-t_2)\Omega]-\sin[2(t_1-t_2)\Omega],$$

$$C_{21}=i(1-2\rho_B^{00})\cos[2(t_1-t_2)\Omega]+\sin[2(t_1-t_2)\Omega],$$

$$C_{22}=\cos[2(t_1-t_2)\Omega]-i(1-2\rho_B^{00})\sin[2(t_1-t_2)\Omega],$$

$$C_{33}=1, \tag{28}$$

where we have omitted the time dependencies for brevity. This can be inserted in the expression for the second-order Lamb-shift Hamiltonian in Eq. (19) to yield

$$\boldsymbol{H}_{\text{eff}}^{\tau,2}=\frac{2\lambda^2}{\Omega-\omega}\{1-\text{sinc}[2\tau(\Omega-\omega)]\}\left[\left(\rho_B^{00}-\frac{1}{2}\right)1_S-\frac{1}{2}\sigma_S^z\right], \tag{29}$$

which commutes with the system Hamiltonian.

The second-order dissipative terms must be calculated from the dissipative parts of Eq. (19), where we obtain for the nonvanishing matrix elements of the dampening matrix $\gamma_{00,00}^{\tau,2}=4\lambda^2\tau(1-\rho_B^{00})\rho_B^{00}$, $\gamma_{00,11}^{\tau,2}=-4\lambda^2\tau(1-\rho_B^{00})\rho_B^{00}$, $\gamma_{11,00}^{\tau,2}=-4\lambda^2\tau(1-\rho_B^{00})\rho_B^{00}$, $\gamma_{11,11}^{\tau,2}=4\lambda^2\tau(1-\rho_B^{00})\rho_B^{00}$, $\gamma_{01,01}^{\tau,2}=4\lambda^2\tau\rho_B^{00}\,\text{sinc}^2[\tau(\Omega-\omega)]$, and $\gamma_{10,10}^{\tau,2}=4\lambda^2\tau(1-\rho_B^{00})\text{sinc}^2[\tau(\Omega-\omega)]$, which shows (e.g., by the Gershgorin circle theorem [25]) that $\gamma_{ab,cd}$ is positive semidefinite. The solution of the coarse-graining master equation $\dot{\boldsymbol{\rho}}_S^{\tau}(t)=\boldsymbol{\mathcal{L}}^{\tau}\boldsymbol{\rho}_S^{\tau}(t)$ can be conveniently obtained by exploiting that diagonal and off-diagonal matrix elements decouple. From the diagonal equations

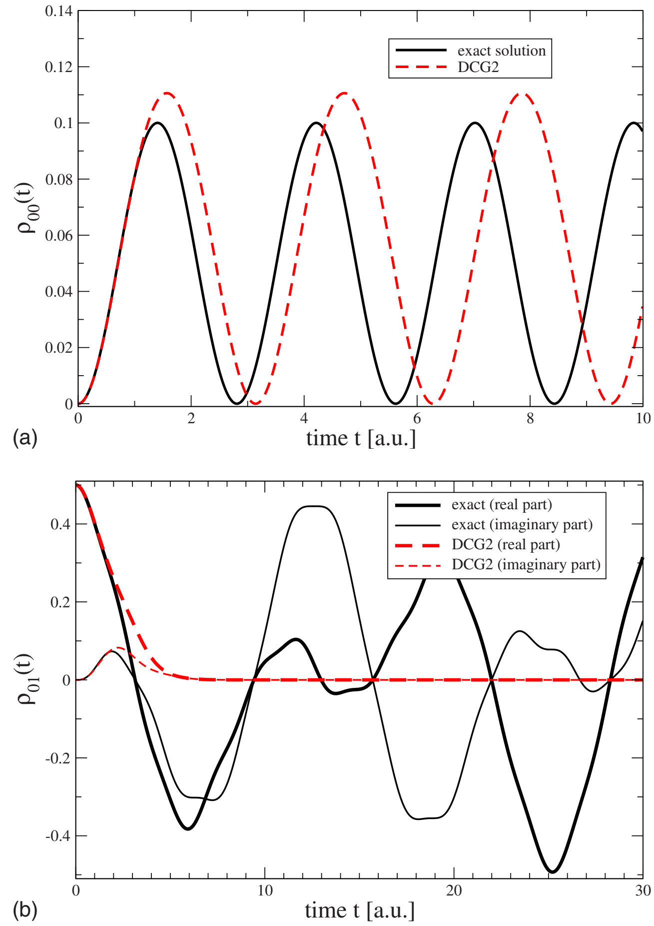

FIG. 1. (Color online) Comparison of exact (solid black line) and DCG2 (dashed red line) solutions for the (a) diagonal and (b) off-diagonal matrix elements of the density matrix. Imaginary parts are displayed with thin lines. Naturally, the exact solution displays complete recurrences. For the diagonal matrix elements, this feature is well reproduced by the DCG2 approach, whereas for the off-diagonals only the short-time dynamics is well approximated. The other parameters have been chosen as follows: $\lambda=0.25$, $\omega=1.0$, $\Omega=2.0$, and $\rho_B^{00}=0.5$.

$$\begin{aligned}\dot{\boldsymbol{\rho}}_S^{00}(t) &= \gamma_{01,01}^{\tau,2}\boldsymbol{\rho}_S^{11}(t)-\gamma_{10,10}^{\tau,2}\boldsymbol{\rho}_S^{00}(t)\\ &= \gamma_{01,01}^{\tau,2}-[\gamma_{01,01}^{\tau,2}+\gamma_{10,10}^{\tau,2}]\boldsymbol{\rho}_S^{00}(t)\\ &= 4\lambda^2\tau\rho_B^{00}\,\text{sinc}^2[\tau(\Omega-\omega)]\\ &\quad -4\lambda^2\tau\,\text{sinc}^2[\tau(\Omega-\omega)]\boldsymbol{\rho}_S^{00}(t),\end{aligned} \tag{30}$$

we obtain the solution at $\tau=t$,

$$\begin{aligned}\langle 0|\boldsymbol{\rho}_S^t(t)|0\rangle &= \exp\left\{-4\frac{\lambda^2}{(\Omega-\omega)^2}\sin^2[t(\Omega-\omega)]\right\}\rho_S^{00}(0)\\ &\quad+\left[1-\exp\left\{-\frac{4\lambda^2\sin^2[t(\Omega-\omega)]}{(\Omega-\omega)^2}\right\}\right]\rho_B^{00},\end{aligned}$$

which does admit for complete recurrences of the populations; see Fig. 1(a).

For the off-diagonal equation

$$\dot{\boldsymbol{\rho}}_{\mathbf{S}}^{01}(t) = \left[\gamma^{\tau,2}_{00,11} - \frac{1}{2}(\gamma^{\tau,2}_{00,00} + \gamma^{\tau,2}_{01,01} + \gamma^{\tau,2}_{10,10} + \gamma^{\tau,2}_{11,11}) + i(\langle 1|\boldsymbol{H}^{\tau,1}_{\mathrm{eff}}|1\rangle + \langle 1|\boldsymbol{H}^{\tau,2}_{\mathrm{eff}}|1\rangle - \langle 0|\boldsymbol{H}^{\tau,1}_{\mathrm{eff}}|0\rangle - \langle 0|\boldsymbol{H}^{\tau,2}_{\mathrm{eff}}|0\rangle) \right] \boldsymbol{\rho}_{\mathbf{S}}^{01}(t)$$
$$= \left\{ -8\lambda^2 \tau \rho_{\mathrm{B}}^{00}(1-\rho_{\mathrm{B}}^{00}) - 2\lambda^2 \tau \,\mathrm{sinc}^2[\tau(\Omega-\omega)] + i\left(\frac{2\lambda^2\{1-\mathrm{sinc}[2\tau(\Omega-\omega)]\}}{\Omega-\omega} + 2\lambda(1-2\rho_{\mathrm{B}}^{00}) \right) \right\} \boldsymbol{\rho}_{\mathbf{S}}^{01}(t), \tag{31}$$

we obtain the solution

$$\langle 0|\boldsymbol{\rho}_{\mathbf{S}}^{t}(t)|1\rangle = e^{-8\lambda^2 t^2 \rho_{\mathrm{B}}^{00}(1-\rho_{\mathrm{B}}^{00}) - 2\lambda^2 t^2 \,\mathrm{sinc}^2[t(\Omega-\omega)]} \times e^{+it[2\lambda^2\{1-\mathrm{sinc}[2t(\Omega-\omega)]\}/(\Omega-\omega)+2\lambda(1-2\rho_{\mathrm{B}}^{00})]} \boldsymbol{\rho}_{\mathbf{S}}^{01}(0), \tag{32}$$

where we will generally observe a decay whenever $\rho_{\mathrm{B}}^{00}(1-\rho_{\mathrm{B}}^{00}) \neq 0$; see Fig. 1(b).

B. DCG4 for two spins

In order to keep the calculations for DCG4 very simple, we consider

$$H_{\mathrm{S}} = \omega \sigma_{\mathrm{S}}^{z}, \quad H_{\mathrm{B}} = \Omega \sigma_{\mathrm{B}}^{z}, \quad H_{\mathrm{SB}} = \lambda \sigma_{\mathrm{S}}^{x} \otimes \sigma_{\mathrm{B}}^{z}, \tag{33}$$

where also here the coupling operators are Hermitian. In this case, the bath correlation functions are all time independent, which enables a convenient calculation of the Liouvillian matrix elements. The example is of course a bit trivial, since the exact solution for the reduced density matrix does not depend on Ω. Note, however, that unlike the pure dephasing limit considered in [26] this case still holds some time dependence that can be found in the system operator in the interaction picture.

The exact solution can be calculated by exponentiating the complete Hamiltonian and tracing out the second spin in the solution for the density matrix as in Sec. III A. In a similar manner we determine the DCG1, DCG2, DCG3, and DCG4 solutions by directly determining the 4×4 Liouvillian matrix as described in Sec. II D (not shown). The solution is then obtained by exponentiating the Liouvillian. The resulting solution for the diagonals is displayed in Fig. 2(a) and that for the off-diagonals in Fig. 2(b).

C. Spin-boson model

We consider a single system spin coupled to a bath of bosonic modes ($\omega_k > 0$),

$$H_{\mathrm{S}} = \frac{\varepsilon_d}{2}(1-\sigma^z), \quad H_{\mathrm{B}} = \sum_k \omega_k \left(b_k^\dagger b_k + \frac{1}{2} \right),$$

$$H_{\mathrm{SB}} = \lambda A \otimes \left[\sum_k h_k b_k + h_k^* b_k^\dagger \right], \tag{34}$$

where for simplicity we have restricted ourselves to the case of single-operator coupling, and the operator $A = A^\dagger$ will be specified later on.

We will consider a thermalized initial bath density matrix

$$\rho_{\mathrm{B}}^{0} = \frac{e^{-\beta H_{\mathrm{B}}}}{\mathrm{Tr}_{\mathrm{B}}\{e^{-\beta H_{\mathrm{B}}}\}}, \tag{35}$$

where $\beta = (k_{\mathrm{B}} T)^{-1}$ denotes the inverse reservoir temperature.

1. Bath correlation functions

We evaluate the traces in the correlation functions in Eq. (12) in Fock space, where bath density matrix (35) is diago-

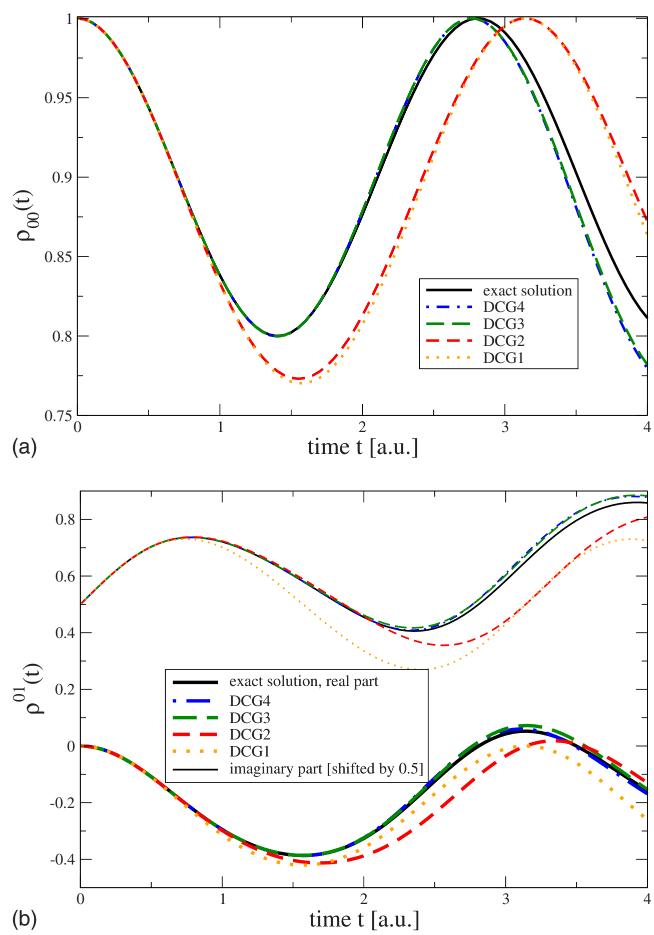

FIG. 2. (Color online) Comparison of exact (solid black line) and DCG1 (dotted orange line), DCG2 (dashed red line), DCG3 (long-dashed green line), and DCG4 solutions (dot-dashed line) for the (a) diagonal and (b) off-diagonal matrix elements of the density matrix. For small times, DCG4 is superior to the coarse-graining methods of smaller accuracy. By construction, the exact solution shows complete recurrences. For larger times, all coarse-graining methods also display recurrences but all of them miss the exact solution (not shown). Parameters have been chosen as $\lambda = 0.5$, $\omega = 1$, and $\rho_{\mathrm{B}}^{00} = 1$.

nal. By doing so it becomes obvious that the number of creation and annihilation operators in each term of the bath-bath correlation functions must be balanced for all modes to obtain a nonvanishing result. Therefore, we conclude (since only one operator is involved, we may omit the indices) that $C(t_1)=0=C(t_1,t_2,t_3)$. In the interaction picture, the annihilation and creation operators transform according to $\boldsymbol{b_k}(t)=e^{+iH_B t}b_k e^{-iH_B t}=e^{-i\omega_k t}b_k$ and the Hermitian conjugate, respectively.

The second-order correlation function then evaluates to

$$C(t_1,t_2)=\frac{1}{2\pi}\int_0^\infty d\omega G(\omega)\{n(\omega)e^{+i\omega(t_1-t_2)} + [1+n(\omega)]e^{-i\omega(t_1-t_2)}\} = \frac{1}{2\pi}\int_{-\infty}^{+\infty}\frac{G(|\omega|)}{|e^{\beta\omega}-1|}e^{+i\omega(t_1-t_2)}d\omega, \tag{36}$$

where the bosonic occupation number is given by $n(\omega)=\frac{1}{e^{\beta\omega}-1}$. In the above equation, we have assumed a quasicontinuous spectral density $G(\omega)=2\pi\Sigma_k|h_k|^2\delta(\omega-\omega_k)$ to convert the sum into an integral. When we parametrize the spectral density as

$$G(\omega)=G_0\omega^S e^{-\omega/\omega_c}, \tag{37}$$

where ω_c denotes a cutoff frequency and the parameter S governs the slope at $\omega=0$, we can obtain an analytic solution for the correlation function [27,28]

$$C(t_1,t_2)=\frac{G_0\Gamma(1+S)}{2\pi\beta^{1+S}}\left[\zeta\left(1+S,\frac{1}{\beta\omega_c}+i\frac{(t_1-t_2)}{\beta}\right) + \zeta\left(1+S,1+\frac{1}{\beta\omega_c}-i\frac{(t_1-t_2)}{\beta}\right)\right] \tag{38}$$

in terms of generalized Riemann zeta functions $\zeta(x,y)$.

The next nonvanishing correlation function is fourth order, where we obtain

$$C(t_1,t_2,t_3,t_4)=C(t_2,t_3)C(t_1,t_4)+C(t_1,t_3)C(t_2,t_4) + C(t_1,t_2)C(t_3,t_4), \tag{39}$$

which can, for example, be obtained using Wick's theorem (for a special case see also Eq. (61) of [16]).

2. Pure dephasing

The case of pure dephasing $A=\sigma^z$ is exactly solvable [29,30] and it is known that DCG2 already yields the exact result [20]. The exact solution predicts time-independent diagonal matrix elements and a decay of the off-diagonal matrix element according to (in the interaction picture, cf. Eq. (82) of [30] in the limit of a continuous bath spectrum)

$$\boldsymbol{\rho}_{01}(t)=e^{-\Gamma(t)}\boldsymbol{\rho}_{01}(0),$$

$$\Gamma(t)=\frac{8\lambda^2}{2\pi}\int_0^\infty G(\omega)\frac{\sin^2(\omega t/2)}{\omega^2}\coth\left[\frac{\beta\omega}{2}\right]d\omega, \tag{40}$$

where the additional factor of $\frac{1}{2\pi}$ in comparison to [20] results from a different definition of the spectral density $G(\omega)$.

By taking the time derivative of the exact solution density matrix, we obtain a closed master equation that is not of Lindblad form (not even with time-dependent coefficients) but nevertheless must—as it is exact—preserve positivity. Hence, one would regard this case as truly non-Markovian [22]. The corresponding steady state is also derived by the equation of motion method in Appendix A. For pure dephasing we have $\boldsymbol{A}(t)=A=\sigma^z$. We observe a decoupled evolution of diagonal and off-diagonal matrix elements of the density matrix.

For the second-order contribution we have [using $\Theta(t_1-t_2)+\Theta(t_2-t_1)=1$] from Eq. (13)

$$\mathcal{T}_2^\tau\boldsymbol{\rho}_S^0=\int_0^\tau C(t_1,t_2)[\sigma^z\boldsymbol{\rho}_S^0\sigma^z-\boldsymbol{\rho}_S^0]dt_1dt_2, \tag{41}$$

from which we obtain

$$\langle 0|\mathcal{T}_2^\tau\boldsymbol{\rho}_S^0|0\rangle=\langle 1|\mathcal{T}_2^\tau\boldsymbol{\rho}_S^0|1\rangle=0,$$

$$\langle 0|\mathcal{T}_2^\tau\boldsymbol{\rho}_S^0|1\rangle=-2\int_0^\tau C(t_1,t_2)dt_1dt_2\boldsymbol{\rho}_S^{01} = -\frac{8}{2\pi}\int_0^\infty G(\omega)\frac{\sin^2(\omega\tau/2)}{\omega^2}\coth\left[\frac{\beta\omega}{2}\right]d\omega\boldsymbol{\rho}_S^{01},$$

which leads to the same exponential decay as with exact solution (40); i.e., as noted earlier [20], DCG2 yields the exact solution in this case. Note that this example demonstrates explicitly that the DCG2 solution cannot be generally written as the solution of a single Lindblad-type master equation with time-dependent coefficients, such that it should be classified as non-Markovian [22].

Using the relation

$$0=+\Theta(t_4-t_3)\Theta(t_3-t_2)\Theta(t_2-t_1)+\Theta(t_3-t_4)\Theta(t_2-t_1) + \Theta(t_1-t_2)\Theta(t_2-t_3)\Theta(t_3-t_4)-\Theta(t_2-t_3)\Theta(t_3-t_4) - \Theta(t_3-t_2)\Theta(t_2-t_1), \tag{42}$$

we obtain for the fourth-order contribution

$$\langle 0|\mathcal{T}_4^\tau\boldsymbol{\rho}_S^0|0\rangle=\langle 1|\mathcal{T}_4^\tau\boldsymbol{\rho}_S^0|1\rangle=0,$$

$$\langle 0|\mathcal{T}_4^\tau\boldsymbol{\rho}_S^0|1\rangle=2\boldsymbol{\rho}_S^{01}\int_0^\tau dt_1dt_2dt_3dt_4C(t_1,t_2,t_3,t_4) \times[\Theta(t_3-t_2)\Theta(t_2-t_1)+\Theta(t_2-t_3)\Theta(t_3-t_4)] = 2\int_0^\tau dt_1dt_2dt_3dt_4C(t_1,t_2)C(t_3,t_4)\boldsymbol{\rho}_S^{01}, \tag{43}$$

where we have exploited the symmetries of the fourth-order correlation functions under exchange of the arguments and the relation

$$2=[+\Theta(t_2-t_3)\Theta(t_3-t_4)+\Theta(t_3-t_2)\Theta(t_2-t_1) + \Theta(t_1-t_2)\Theta(t_2-t_4)+\Theta(t_2-t_1)\Theta(t_1-t_3) + \Theta(t_3-t_2)\Theta(t_2-t_4)+\Theta(t_2-t_3)\Theta(t_3-t_1) + \Theta(t_4-t_1)\Theta(t_1-t_2)+\Theta(t_1-t_4)\Theta(t_4-t_3)$$

$$+\Theta(t_3-t_4)\Theta(t_4-t_2)+\Theta(t_4-t_3)\Theta(t_3-t_1)$$
$$+\Theta(t_1-t_4)\Theta(t_4-t_2)+\Theta(t_4-t_1)\Theta(t_1-t_3)]. \quad (44)$$

The nonvanishing off-diagonal contribution has to be compared with the counterterm arising from the second order,

$$\frac{1}{2}\langle 0|\mathcal{T}_2^\tau\mathcal{T}_2^\tau\boldsymbol{\rho}_{\mathbf{S}}^0|1\rangle = \frac{1}{2}\left[-2\int_0^\tau C(t_1,t_2)dt_1dt_2\right]^2\boldsymbol{\rho}_{\mathbf{S}}^{01}$$
$$=2\left[\int_0^\tau C(t_1,t_2)dt_1dt_2\right]\times\left[\int_0^\tau C(t_3,t_4)dt_3dt_4\right]\boldsymbol{\rho}_{\mathbf{S}}^{01}. \quad (45)$$

Since the diagonal elements of the density matrix are neither affected by $\mathcal{T}_2^\tau$ nor by $\mathcal{T}_4^\tau$, we conclude that we have for pure dephasing

$$\mathcal{T}_4^\tau = \frac{1}{2}\mathcal{T}_2^\tau\mathcal{T}_2^\tau, \quad (46)$$

such that DCG4 will yield the same result as DCG2. Since DCG2 is already exact for this case, this cancellation is a strong indicator of the correctness of our fourth-order correlation function (39).

3. Dissipation

We are now in a position to apply DCG to more interesting coupling operators (picking up a time dependence in the interaction picture) that also affect the evolution of the diagonal elements of the density matrix. Transforming $A=\sigma^x$ into the interaction picture, we obtain $\boldsymbol{A}(t)=\cos(\varepsilon_d t)\sigma^x+\sin(\varepsilon_d t)\sigma^y$. Inserting this result we find for the second-order term in Eq. (13)

$$\langle 0|\mathcal{T}_2^\tau[\boldsymbol{\rho}_{\mathbf{S}}]|0\rangle = \int_0^\tau dt_1dt_2C(t_1,t_2)[-e^{-i\varepsilon_d(t_1-t_2)}\boldsymbol{\rho}_{\mathbf{S}}^{00} + e^{+i\varepsilon_d(t_1-t_2)}\boldsymbol{\rho}_{\mathbf{S}}^{11}],$$

$$\langle 0|\mathcal{T}_2^\tau[\boldsymbol{\rho}_{\mathbf{S}}]|1\rangle = \int_0^\tau dt_1dt_2C(t_1,t_2)[-\Theta(t_2-t_1)e^{+i\varepsilon_d(t_1-t_2)}\boldsymbol{\rho}_{\mathbf{S}}^{01} - \Theta(t_1-t_2)e^{-i\varepsilon_d(t_1-t_2)}\boldsymbol{\rho}_{\mathbf{S}}^{01} + e^{-i\varepsilon_d(t_1+t_2)}\boldsymbol{\rho}_{\mathbf{S}}^{10}] \quad (47)$$

and similarly for the other terms, such that by arranging the matrix elements of the 2×2 density matrix in a four-dimensional vector as $(\boldsymbol{\rho}_{\mathbf{S}}^{00},\boldsymbol{\rho}_{\mathbf{S}}^{01},\boldsymbol{\rho}_{\mathbf{S}}^{10},\boldsymbol{\rho}_{\mathbf{S}}^{11})$, we find the matrix elements of the corresponding 4×4 superoperator to be

$$\mathcal{T}_2^\tau = \int_0^\tau C(t_1,t_2)\begin{pmatrix} -e^{-i\varepsilon_d(t_1-t_2)} & 0 & 0 & +e^{+i\varepsilon_d(t_1-t_2)} \\ 0 & -e^{-i\varepsilon_d|t_1-t_2|} & +e^{-i\varepsilon_d(t_1+t_2)} & 0 \\ 0 & +e^{+i\varepsilon_d(t_1+t_2)} & -e^{+i\varepsilon_d|t_1-t_2|} & 0 \\ +e^{-i\varepsilon_d(t_1-t_2)} & 0 & 0 & -e^{+i\varepsilon_d(t_1-t_2)} \end{pmatrix}dt_1dt_2, \quad (48)$$

such that we observe a decoupled evolution of diagonal and off-diagonal matrix elements. Defining

$$m_{11}(\tau) \equiv (\mathcal{T}_2^\tau)_{11} = -\frac{\tau^2}{2\pi}\int_{-\infty}^{+\infty}\frac{G(|\omega|)}{|e^{\beta\omega}-1|}\mathrm{sinc}^2\left[(\omega-\varepsilon_d)\frac{\tau}{2}\right]d\omega,$$

$$m_{14}(\tau) \equiv (\mathcal{T}_2^\tau)_{14} = +\frac{\tau^2}{2\pi}\int_{-\infty}^{+\infty}\frac{G(|\omega|)}{|e^{\beta\omega}-1|}\mathrm{sinc}^2\left[(\omega+\varepsilon_d)\frac{\tau}{2}\right]d\omega,$$

$$m_{41}(\tau) \equiv (\mathcal{T}_2^\tau)_{41} = -m_{11}(\tau),$$

$$m_{44}(\tau) \equiv (\mathcal{T}_2^\tau)_{44} = -m_{14}(\tau), \quad (49)$$

we obtain the second-order solution for the diagonals (using trace conservation),

$$\rho_{00}^\tau(\tau) = \rho_{00}^0\exp\{\lambda^2[m_{11}(\tau)-m_{14}(\tau)]\} + \frac{1-\exp\{\lambda^2[m_{11}(\tau)-m_{14}(\tau)]\}}{1-\frac{m_{11}(\tau)}{m_{14}(\tau)}}. \quad (50)$$

In Eq. (49) it is already obvious that for finite times τ all frequencies will contribute to the matrix elements $m_{ij}(\tau)$, in contrast to the Markov approximation, where only $G(\varepsilon_d)$ is relevant. Using the fact that the bandfilter sinc functions transform into Dirac delta functions in Eq. (24), we can perform the limit $\tau\to\infty$ to obtain the steady state

$$\rho_{00}^\infty = \frac{1}{1+e^{-\beta\varepsilon_d}}, \quad (51)$$

which corresponds to the thermalized system density matrix that is consistent with our expectations; compare also Appendix A. The same stationary state can also be obtained by using the method of equation of motion and truncating correlations at second order between system and reservoir.

The Markovian limit is obtained by using

$$m_{11}^{\mathrm{MK}}(t) = t \lim_{\tau\to\infty} \frac{1}{\tau} m_{11}(\tau) = -tG(|\varepsilon_d|)|n(+\varepsilon_d)|,$$

$$m_{14}^{\mathrm{MK}}(t) = t \lim_{\tau\to\infty} \frac{1}{\tau} m_{14}(\tau) = +tG(|\varepsilon_d|)|n(-\varepsilon_d)|, \quad (52)$$

where we have again used identity (24) in Eq. (49). Evidently, the above equation leads to the same steady state as Born-Markov approximation (51).

By virtue of Eq. (42) and using $C(t_1,t_2,t_3,t_4) = [C(t_4,t_3,t_2,t_1)]^*$, we obtain for the diagonal part

$$\begin{aligned}\langle 0|\mathcal{T}_4^\tau \boldsymbol{\rho}_{\mathrm{S}}^0|0\rangle &= 2\int_0^\tau \mathrm{Re}\{C(t_1,t_2,t_3,t_4)e^{-i\varepsilon_d(t_1-t_2+t_3-t_4)}\} \\ &\quad\times\Theta(t_2-t_3)\Theta(t_3-t_4)dt_1dt_2dt_3dt_4\boldsymbol{\rho}_{\mathrm{S}}^{00} \\ &\quad-2\int_0^\tau \mathrm{Re}\{C(t_1,t_2,t_3,t_4)e^{+i\varepsilon_d(t_1-t_2+t_3-t_4)}\} \\ &\quad\times\Theta(t_2-t_3)\Theta(t_3-t_4)dt_1dt_2dt_3dt_4\boldsymbol{\rho}_{\mathrm{S}}^{11} \\ &\equiv p_{11}(\tau)\boldsymbol{\rho}_{\mathrm{S}}^{00} + p_{14}(\tau)\boldsymbol{\rho}_{\mathrm{S}}^{11}. \end{aligned} \quad (53)$$

This result has to be combined with the counterterm arising from the squared second-order contribution. Defining

$$\begin{aligned}\tilde{p}_{11}(\tau) &= \lambda^2 m_{11}(\tau) - \frac{\lambda^4}{2}[m_{11}(\tau)m_{11}(\tau) + m_{14}(\tau)m_{41}(\tau)] \\ &\quad+\lambda^4 p_{11}(\tau), \\ \tilde{p}_{14}(\tau) &= \lambda^2 m_{14}(\tau) - \frac{\lambda^4}{2}[m_{11}(\tau)m_{14}(\tau) + m_{14}(\tau)m_{44}(\tau)] \\ &\quad+\lambda^4 p_{14}(\tau), \end{aligned} \quad (54)$$

we therefore obtain the fourth-order solution

$$\rho_{00}^\tau(\tau) = \rho_{00}^0 \exp[\tilde{p}_{11}(\tau) - \tilde{p}_{14}(\tau)] + \frac{1-\exp[\tilde{p}_{11}(\tau) - \tilde{p}_{14}(\tau)]}{1 - \dfrac{\tilde{p}_{11}(\tau)}{\tilde{p}_{14}(\tau)}}. \quad (55)$$

A general exact solution is unfortunately not available for this case. However, it is interesting to note that when considering the *Markov limit* $\beta=0$, $\omega_c\to\infty$, and $S=0$ (where the Markov approximation becomes exact), the correlation function (36) becomes a δ function and we see that in this limit, the fourth-order term is canceled by the squared second-order counterterm. For comparison, we plot Born-Markov solution, DCG2, and DCG4 solutions in Fig. 3.

For the dissipative spin-boson model and Ohmic dissipation ($S=1$), one obtains an exponential decay of the expectation value $\langle\sigma^x\rangle(t)$ in the long-time limit [31] (note the rotations $\sigma^z\to\sigma^x$ and $\sigma^x\to-\sigma^z$). This corresponds to a decay of the off-diagonal matrix elements and is of course also reproduced by the DCG approach.

D. Fano-Anderson model

We consider the Fano-Anderson model [32,33]: two leads that are connected by a single quantum dot, through which electrons may tunnel from one lead to the other. The Hamiltonian is given by

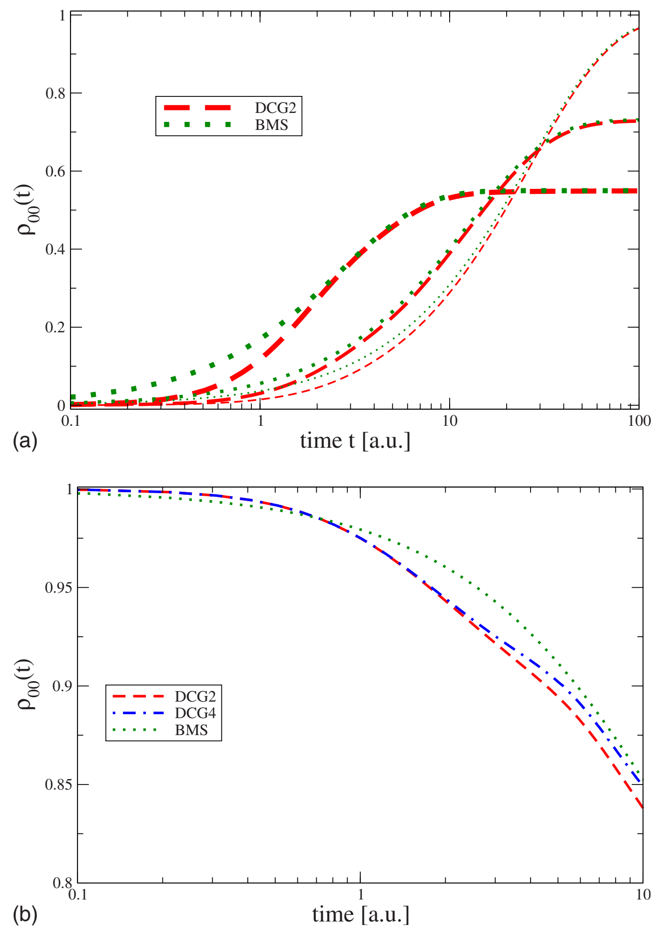

FIG. 3. (Color online) Comparison of DCG2 (dashed red line), DCG4 (dot-dashed blue line), and BMS (dotted green line) approximations to the dissipative spin-boson model. In figure (a) we consider different temperatures $\beta=0.2\varepsilon_d$ (bold line), $\beta=1.0\varepsilon_d$ (medium-thickness line), and $\beta=5.0\varepsilon_d$ (thin line) in the weak-coupling limit $\lambda^2=0.1$ and we see that the steady states always coincide, whereas for small times DCG and BMS solutions differ. In figure (b) we only show the short-time dynamics for $\lambda^2=0.1$ and $\beta=1.0\varepsilon_d$. The other parameters have been chosen as $\varepsilon_d=1$, $\omega_c=1$, $G_0=1$, and $S=1$.

$$H = H_{\mathrm{S}} + H_{\mathrm{B}} + H_{\mathrm{SB}},$$

$$H_{\mathrm{S}} = \varepsilon_d d^\dagger d, \quad H_{\mathrm{B}} = \sum_{ka} \omega_{ka} c_{ka}^\dagger c_{ka},$$

$$H_{\mathrm{SB}} = \lambda \sum_{ka} [t_{ka} d c_{ka}^\dagger - t_{ka}^* d^\dagger c_{ka}] \quad (56)$$

with fermionic operators creating an electron with momentum k in the left or right lead $a\in\{L,R\}$ for $c_{ka}^\dagger$ or in the quantum dot for $d^\dagger$. Due to the fermionic anticommutation relations, the model (56) can be solved exactly, for example, with Green's functions [34,35]. We provide a simplified derivation based on the equation of motion method in Appendix B.

In contrast to our assumptions in Sec. II, the operators d and c_{ka} do not act on separate Hilbert spaces, which is evident from their anticommutation relations $\{d,c_{ka}^\dagger\}=0$. This becomes even more explicit via the decomposition

$$d=|0\rangle\langle 1|\otimes \mathbf{1},$$

$$c_{ka}=[|0\rangle\langle 0|-|1\rangle\langle 1|]\otimes \bar{c}_{ka}, \quad (57)$$

where $|0\rangle$ and $|1\rangle$ denote the empty and filled dot states, respectively, and the fermionic operators $\bar{c}_{ka}$ act only on the (distinct) Fock space of the remaining sites in the leads with $\{\bar{c}_{ka},\bar{c}_{k'a'}^\dagger\}=\delta_{kk'}\delta_{aa'}$. Naturally, the above decomposition obeys the original anticommutation relations such as $\{d,c_{ka}\}=0$ and we conclude for the operators in the interaction Hamiltonian $dc_{ka}^\dagger=-|0\rangle\langle 1|\otimes\bar{c}_{ka}^\dagger$, and $d^\dagger c_{ka}=+|1\rangle\langle 0|\otimes\bar{c}_{ka}$, such that now the new operators commute by construction. Similar decompositions are also possible for systems containing more than one site. We identify

$$A_1=-|0\rangle\langle 1|,\quad A_2=-|1\rangle\langle 0|,$$

$$B_1=\sum_{ka}t_{ka}\bar{c}_{ka}^\dagger,\quad B_2=\sum_{ka}t_{ka}^*\bar{c}_{ka}. \quad (58)$$

We assume that there are no correlations between left and right leads. Here we will just consider the infinite-bias limit (although this is not crucial, it enables an analytic calculation of all integrals). Taking the chemical potentials to plus or minus infinity for the left and right leads, respectively ($\mu_L\to+\infty$ and $\mu_R\to-\infty$), we obtain for the fermionic occupation number

$$\langle\bar{c}_{kL}^\dagger\bar{c}_{kL}\rangle=\frac{1}{e^{\beta(\omega_k-\mu_L)}+1}\to 1,$$

$$\langle\bar{c}_{kR}^\dagger\bar{c}_{kR}\rangle=\frac{1}{e^{\beta(\omega_k-\mu_R)}+1}\to 0. \quad (59)$$

We observe that the coupling operators are non-Hermitian in this case. The correlation functions relevant for the evolution of the diagonal matrix elements can be calculated by using continuum tunneling rates via $\Gamma_a(\omega)\equiv 2\pi\Sigma_k|t_{ka}|^2\delta(\omega-\omega_{ka})$,

$$C_L(t_1-t_2)\equiv C_{12}(t_1,t_2)=\frac{1}{2\pi}\int_{-\infty}^{+\infty}\Gamma_L(\omega)e^{+i\omega(t_1-t_2)}d\omega,$$

$$C_R(t_2-t_1)\equiv C_{21}(t_1,t_2)=\frac{1}{2\pi}\int_{-\infty}^{+\infty}\Gamma_R(\omega)e^{-i\omega(t_1-t_2)}d\omega,$$

$$C_{1212}(t_1,t_2,t_3,t_4)=C_L(t_1-t_2)C_L(t_3-t_4)+C_L(t_1-t_4)C_R(t_3-t_2),$$

$$C_{2121}(t_1,t_2,t_3,t_4)=C_R(t_2-t_1)C_R(t_4-t_3)+C_R(t_4-t_1)C_L(t_2-t_3). \quad (60)$$

From Eq. (13), we can derive the second-order approximation

$$\begin{aligned}\boldsymbol{\mathcal{T}}_2^\tau\boldsymbol{\rho}_{\mathbf{S}}^0=&\int_0^\tau dt_1dt_2[-C_{21}(t_1,t_2)\Theta(t_2-t_1)\boldsymbol{\rho}_{\mathbf{S}}^0\boldsymbol{A}_1^\dagger(t_1)\boldsymbol{A}_2^\dagger(t_2)-C_{12}(t_1,t_2)\Theta(t_2-t_1)\boldsymbol{\rho}_{\mathbf{S}}^0\boldsymbol{A}_2^\dagger(t_1)\boldsymbol{A}_1^\dagger(t_2)+C_{21}(t_1,t_2)\boldsymbol{A}_1(t_2)\boldsymbol{\rho}_{\mathbf{S}}^0\boldsymbol{A}_1^\dagger(t_1)\\&+C_{12}(t_1,t_2)\boldsymbol{A}_2(t_2)\boldsymbol{\rho}_{\mathbf{S}}^0\boldsymbol{A}_2^\dagger(t_1)-C_{12}(t_1,t_2)\Theta(t_1-t_2)\boldsymbol{A}_1(t_1)\boldsymbol{A}_2(t_2)\boldsymbol{\rho}_{\mathbf{S}}^0-C_{21}(t_1,t_2)\Theta(t_1-t_2)\boldsymbol{A}_2(t_1)\boldsymbol{A}_1(t_2)\boldsymbol{\rho}_{\mathbf{S}}^0]\\=&\int_{-\infty}^{+\infty}\frac{d\omega}{2\pi}\Gamma_R(\omega)\int_0^\tau dt_1dt_2e^{-i(\omega-\varepsilon_d)(t_1-t_2)}[-\boldsymbol{\rho}_{\mathbf{S}}^0|1\rangle\langle 1|\Theta(t_2-t_1)+|0\rangle\langle 1|\boldsymbol{\rho}_{\mathbf{S}}^0|1\rangle\langle 0|-|1\rangle\langle 1|\boldsymbol{\rho}_{\mathbf{S}}^0\Theta(t_1-t_2)]\\&+\int_{-\infty}^{+\infty}\frac{d\omega}{2\pi}\Gamma_L(\omega)\int_0^\tau dt_1dt_2e^{+i(\omega-\varepsilon_d)(t_1-t_2)}[-\boldsymbol{\rho}_{\mathbf{S}}^0|0\rangle\langle 0|\Theta(t_2-t_1)+|1\rangle\langle 0|\boldsymbol{\rho}_{\mathbf{S}}^0|0\rangle\langle 1|-|0\rangle\langle 0|\boldsymbol{\rho}_{\mathbf{S}}^0\Theta(t_1-t_2)],\end{aligned} \quad (61)$$

from which we can infer the matrix elements of the second-order Liouvillian via $\boldsymbol{\mathcal{L}}_2^\tau\boldsymbol{\rho}_{\mathbf{S}}^0=\frac{1}{\tau}\boldsymbol{\mathcal{T}}_2^\tau\boldsymbol{\rho}_{\mathbf{S}}^0$. The Born-Markov secular approximation is obtained by the Liouvillian $\boldsymbol{\mathcal{L}}_2^\infty$ with the help of Eq. (24).

When we parametrize the tunneling rates by Lorentzians [36]

$$\Gamma_R(\omega)=\frac{\Gamma_R^0\delta_R^2}{(\omega-\epsilon_R)^2+\delta_R^2},\quad \Gamma_L(\omega)=\frac{\Gamma_L^0\delta_L^2}{(\omega-\epsilon_L)^2+\delta_L^2}, \quad (62)$$

we obtain an analytic expression for the bath correlation functions in terms of a single decaying exponential,

$$C_R(t)=\frac{\Gamma_R^0\delta_R}{2}e^{-|t|\delta_R+i\epsilon_R t},\quad C_L(t)=\frac{\Gamma_L^0\delta_L}{2}e^{-|t|\delta_L+i\epsilon_L t}, \quad (63)$$

such that we can analytically calculate the matrix elements of $\mathcal{T}_2^\tau$ that govern the evolution of the diagonals

$$\begin{pmatrix} m_{11}(\tau) & m_{14}(\tau) \\ m_{41}(\tau) & m_{44}(\tau) \end{pmatrix} \equiv \int_0^\tau dt_1 dt_2 e^{-i\epsilon_d(t_1-t_2)} \times \begin{pmatrix} -C_L(t_1-t_2) & +C_R(t_1-t_2) \\ +C_L(t_1-t_2) & -C_R(t_1-t_2) \end{pmatrix}. \tag{64}$$

Then, we obtain from $\langle 0|\mathcal{T}_2^\tau \boldsymbol{\rho}_{\mathbf{S}}^0|0\rangle$ for the evolution of the diagonal matrix element

$$\dot{\boldsymbol{\rho}}_{00}^\tau = \lambda^2 \left[\frac{m_{11}(\tau)}{\tau} \boldsymbol{\rho}_{00}^\tau(t) + \frac{m_{14}(\tau)}{\tau} \boldsymbol{\rho}_{11}^\tau(t) \right], \tag{65}$$

where we can exploit trace conservation $\boldsymbol{\rho}_{11}^\tau(t)=1-\boldsymbol{\rho}_{00}^\tau(t)$ (this feature is trivially fulfilled by the coarse-graining approach). Afterward, the above equation can explicitly be solved for

$$\boldsymbol{\rho}_{00}^\tau(t) = \boldsymbol{\rho}_{00}(0)\exp\left\{\lambda^2[m_{11}(\tau)-m_{14}(\tau)]\frac{t}{\tau}\right\} + \frac{1-\exp\left\{\lambda^2[m_{11}(\tau)-m_{14}(\tau)]\frac{t}{\tau}\right\}}{1-\frac{m_{11}(\tau)}{m_{14}(\tau)}}. \tag{66}$$

For the fourth-order contribution we obtain [extensively using $C_{\bar{1}\bar{2}\bar{1}\bar{2}}(t_1,t_2,t_3,t_4)=C_{2121}(t_1,t_2,t_3,t_4)$, $C_{1112}(t_1,t_2,t_3,t_4)=0$, etc.]

$$\begin{aligned}
\mathcal{T}_4^\tau \boldsymbol{\rho}_{\mathbf{S}}^0 = \int_0^\tau dt_1dt_2dt_3dt_4[&+C_{2121}(t_1,t_2,t_3,t_4)\Theta(t_4-t_3)\Theta(t_3-t_2)\Theta(t_2-t_1)\boldsymbol{\rho}_{\mathbf{S}}^0\boldsymbol{A}_1^\dagger(t_1)\boldsymbol{A}_2^\dagger(t_2)\boldsymbol{A}_1^\dagger(t_3)\boldsymbol{A}_2^\dagger(t_4)\\
&+C_{1212}(t_1,t_2,t_3,t_4)\Theta(t_4-t_3)\Theta(t_3-t_2)\Theta(t_2-t_1)\boldsymbol{\rho}_{\mathbf{S}}^0\boldsymbol{A}_2^\dagger(t_1)\boldsymbol{A}_1^\dagger(t_2)\boldsymbol{A}_2^\dagger(t_3)\boldsymbol{A}_1^\dagger(t_4)\\
&-C_{2121}(t_1,t_2,t_3,t_4)\Theta(t_3-t_2)\Theta(t_2-t_1)\boldsymbol{A}_1(t_4)\boldsymbol{\rho}_{\mathbf{S}}^0\boldsymbol{A}_1^\dagger(t_1)\boldsymbol{A}_2^\dagger(t_2)\boldsymbol{A}_1^\dagger(t_3)\\
&-C_{1212}(t_1,t_2,t_3,t_4)\Theta(t_3-t_2)\Theta(t_2-t_1)\boldsymbol{A}_2(t_4)\boldsymbol{\rho}_{\mathbf{S}}^0\boldsymbol{A}_2^\dagger(t_1)\boldsymbol{A}_1^\dagger(t_2)\boldsymbol{A}_2^\dagger(t_3)\\
&+C_{2112}(t_1,t_2,t_3,t_4)\Theta(t_3-t_4)\Theta(t_2-t_1)\boldsymbol{A}_1(t_3)\boldsymbol{A}_2(t_4)\boldsymbol{\rho}_{\mathbf{S}}^0\boldsymbol{A}_1^\dagger(t_1)\boldsymbol{A}_2^\dagger(t_2)\\
&+C_{2121}(t_1,t_2,t_3,t_4)\Theta(t_3-t_4)\Theta(t_2-t_1)\boldsymbol{A}_2(t_3)\boldsymbol{A}_1(t_4)\boldsymbol{\rho}_{\mathbf{S}}^0\boldsymbol{A}_1^\dagger(t_1)\boldsymbol{A}_2^\dagger(t_2)\\
&+C_{1212}(t_1,t_2,t_3,t_4)\Theta(t_3-t_4)\Theta(t_2-t_1)\boldsymbol{A}_1(t_3)\boldsymbol{A}_2(t_4)\boldsymbol{\rho}_{\mathbf{S}}^0\boldsymbol{A}_2^\dagger(t_1)\boldsymbol{A}_1^\dagger(t_2)\\
&+C_{1221}(t_1,t_2,t_3,t_4)\Theta(t_3-t_4)\Theta(t_2-t_1)\boldsymbol{A}_2(t_3)\boldsymbol{A}_1(t_4)\boldsymbol{\rho}_{\mathbf{S}}^0\boldsymbol{A}_2^\dagger(t_1)\boldsymbol{A}_1^\dagger(t_2)\\
&-C_{2121}(t_1,t_2,t_3,t_4)\Theta(t_2-t_3)\Theta(t_3-t_4)\boldsymbol{A}_1(t_2)\boldsymbol{A}_2(t_3)\boldsymbol{A}_1(t_4)\boldsymbol{\rho}_{\mathbf{S}}^0\boldsymbol{A}_1^\dagger(t_1)\\
&-C_{1212}(t_1,t_2,t_3,t_4)\Theta(t_2-t_3)\Theta(t_3-t_4)\boldsymbol{A}_2(t_2)\boldsymbol{A}_1(t_3)\boldsymbol{A}_2(t_4)\boldsymbol{\rho}_{\mathbf{S}}^0\boldsymbol{A}_2^\dagger(t_1)\\
&+C_{1212}(t_1,t_2,t_3,t_4)\Theta(t_1-t_2)\Theta(t_2-t_3)\Theta(t_3-t_4)\boldsymbol{A}_1(t_1)\boldsymbol{A}_2(t_2)\boldsymbol{A}_1(t_3)\boldsymbol{A}_2(t_4)\boldsymbol{\rho}_{\mathbf{S}}^0\\
&+C_{2121}(t_1,t_2,t_3,t_4)\Theta(t_1-t_2)\Theta(t_2-t_3)\Theta(t_3-t_4)\boldsymbol{A}_2(t_1)\boldsymbol{A}_1(t_2)\boldsymbol{A}_2(t_3)\boldsymbol{A}_1(t_4)\boldsymbol{\rho}_{\mathbf{S}}^0].
\end{aligned} \tag{67}$$

The relevant part in above equation for the evolution of the diagonals evaluates by using Eq. (42) to

$$(\mathcal{T}_4^\tau \boldsymbol{\rho}_{\mathbf{S}}^0)_{11} \equiv p_{11}(\tau)\boldsymbol{\rho}_{00}^\tau(t) + p_{14}(\tau)\boldsymbol{\rho}_{11}^\tau(t),$$

$$\begin{aligned}
p_{11}(\tau) = +\int_0^\tau dt_1dt_2dt_3dt_4 e^{-i\varepsilon_d(+t_1-t_2+t_3-t_4)} &\times[C_L(t_1-t_2)C_L(t_3-t_4)+C_L(t_1-t_4)C_R(t_3-t_2)]\\
&\times[\Theta(t_3-t_2)\Theta(t_2-t_1)+\Theta(t_2-t_3)\Theta(t_3-t_4)],
\end{aligned}$$

$$\begin{aligned}
p_{14}(\tau) = -\int_0^\tau dt_1dt_2dt_3dt_4 e^{+i\varepsilon_d(t_1-t_2+t_3-t_4)} &\times[C_R(t_2-t_1)C_R(t_4-t_3)+C_R(t_4-t_1)C_L(t_2-t_3)]\\
&\times[\Theta(t_3-t_2)\Theta(t_2-t_1)+\Theta(t_2-t_3)\Theta(t_3-t_4)],
\end{aligned} \tag{68}$$

where again all integrals can be solved analytically, yielding even lengthier expressions than before.

Together with

$$\langle 0|\mathcal{T}_2^\tau\mathcal{T}_2^\tau\boldsymbol{\rho}_{\mathbf{S}}^0|0\rangle = [m_{11}(\tau)m_{11}(\tau)+m_{14}(\tau)m_{41}(\tau)]\boldsymbol{\rho}_{\mathbf{S}}^{00} + [m_{11}(\tau)m_{14}(\tau)+m_{14}(\tau)m_{44}(\tau)]\boldsymbol{\rho}_{\mathbf{S}}^{11},$$

we obtain from

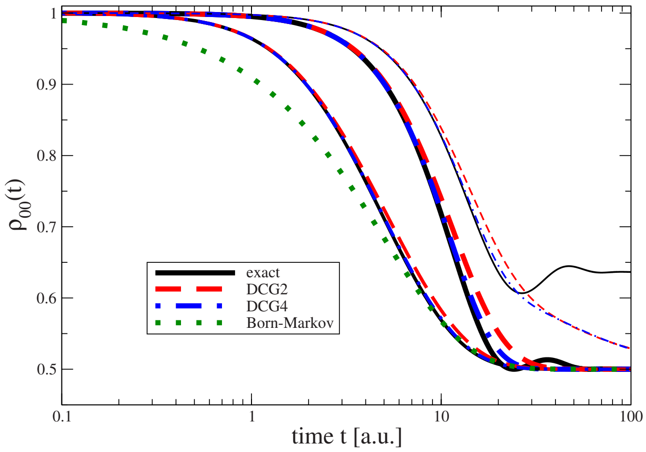

FIG. 4. (Color online) Comparison of exact (solid black line), DCG2 (dashed red line), DCG4 (dot-dashed blue line), and Born-Markov (dotted green line; same for all parameters) solutions for the Fano-Anderson model. The bold lines ($\delta_L=\delta_R=0.1$) show the highly non-Markovian regime, whereas the medium-thickness lines ($\delta_L=\delta_R=1.0$) denote a regime where the Markovian approximation performs comparably well. The thin lines ($\delta_R=2\delta_L=0.1$) demonstrate the failure of the DCG solutions in the large-time limit. The other parameters have been chosen as $\lambda^2=0.1$, $\Gamma_R^0=\Gamma_L^0=1$, and $\varepsilon_R=\varepsilon_d=\varepsilon_L=1$.

$$\lambda^2\mathcal{L}_2^\tau+\lambda^4\mathcal{L}_4^\tau=\frac{\lambda^2}{\tau}\mathcal{T}_2^\tau+\frac{\lambda^4}{\tau}\left(\mathcal{T}_4^\tau-\frac{\tau^2}{2}\mathcal{L}_2^\tau\mathcal{L}_2^\tau\right)$$
$$=\frac{1}{\tau}\left(\lambda^2\mathcal{T}_2^\tau+\lambda^4\mathcal{T}_4^\tau-\frac{\lambda^4}{2}\mathcal{T}_2^\tau\mathcal{T}_2^\tau\right) \qquad (69)$$

the following differential equation for the diagonals:

$$\dot{\boldsymbol{\rho}}_{00}^\tau=\frac{1}{\tau}\Bigg\{\lambda^2 m_{11}(\tau)-\frac{\lambda^4}{2}[m_{11}(\tau)m_{11}(\tau)+m_{14}(\tau)m_{41}(\tau)] + \lambda^4 p_{11}(\tau)\Bigg\}\boldsymbol{\rho}_{00}^\tau(t)+\frac{1}{\tau}\Bigg\{\lambda^2 m_{14}(\tau)-\frac{\lambda^4}{2}[m_{11}(\tau)m_{14}(\tau) + m_{14}(\tau)m_{44}(\tau)]+\lambda^4 p_{14}(\tau)\Bigg\}\boldsymbol{\rho}_{11}^\tau(t). \qquad (70)$$

The above equation can be explicitly solved for $\boldsymbol{\rho}_{00}^\tau(\tau)$ by imposing trace conservation as in Sec. III C. It can be shown analytically that in the flatband limit $\delta_R\to\infty, \delta_L\to\infty$ (where for infinite bias the Markovian approximation becomes exact), the fourth-order correction in the above equation is canceled by the counterterm from the second order for all graining times τ. Moreover, one can also show analytically that the apparent divergence for large graining times $p_{11}\propto\tau^2$ and $p_{14}\propto\tau^2$ is precisely canceled by the fourth-order counter terms arising from the second order.

In contrast, one obtains under the Born-Markov (the secular approximation has no effect for this particular example) approximation the solution

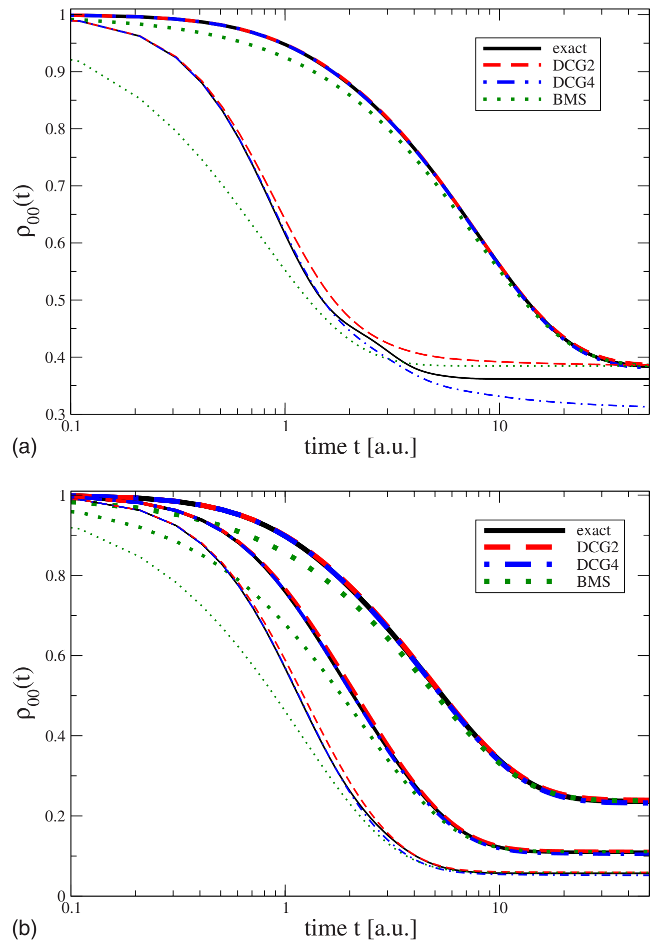

FIG. 5. (Color online) Comparison of exact (solid black line), DCG2 (dashed red line), DCG4 (dot-dashed blue line), and Born-Markov (dotted green line) solutions for the Fano-Anderson model. In figure (a), we have considered symmetric maximum tunneling rates $\Gamma_L^0=\Gamma_R^0=1$ for the weak-coupling limit $\lambda^2=0.1$ (bold lines) and the strong-coupling limit $\lambda^2=1.0$ (thin lines). It is visible that the steady state of BMS and DCG2 solutions does not depend on the coupling strength and in the strong-coupling limit, the steady state of DCG4 might actually be worse than that of DCG2. In figure (b), we have used $\lambda^2=0.1$ and $\Gamma_R^0=1.0$ and varied the left maximum tunneling rate as $\Gamma_L^0=2.0$ (bold line), $\Gamma_L^0=5.0$ (medium-thickness line), and $\Gamma_L^0=10.0$ (thin line). For small times, DCG4 always yields a better result than DCG2 and both DCG solutions are better than the BMS approximation. The latter performs particularly bad for small times as expected. The other parameters have (in both figures) been chosen as $\delta_R=1$, $\delta_L=2$, $\varepsilon_R=\varepsilon_L=0$, and $\varepsilon_d=1$.

$$\boldsymbol{\rho}_{00}(\tau)=\frac{\Gamma_R(\varepsilon_d)}{\Gamma_L(\varepsilon_d)+\Gamma_R(\varepsilon_d)}\left(1-e^{-\lambda^2[\Gamma_L(\varepsilon_d)+\Gamma_R(\varepsilon_d)]\tau}\right)+\boldsymbol{\rho}_{00}(0)e^{-\lambda^2[\Gamma_L(\varepsilon_d)+\Gamma_R(\varepsilon_d)]\tau}, \qquad (71)$$

which has been derived using Eq. (52) and identity (24). From Lorentzian tunneling rates (62) we see that the Markovian solution is completely independent of the width of the tunneling rates δ_R and δ_L; see also Fig. 4. Especially for small widths δ_R and δ_L correlation functions (63) decay very slowly and we also observe a large difference between Born-

Markov and exact solutions, whereas the DCG solutions perform comparably well. With the exact solution from Appendix B we plot the Born-Markov solution, and DCG2 as well as DCG4 solutions in Fig. 5 for varying coupling strengths as well as for different model symmetries.

IV. SUMMARY

The dynamical coarse-graining approach has been extended to higher orders. By performing the derivation in the interaction picture, we have directly demonstrated that the DCG solution must approximate the exact solution by construction for small times. This has been confirmed by several examples. Interestingly, the DCG method even reproduced the complete recurrences of the diagonal density matrix elements in case of small reservoirs. For continuous reservoirs, the short-time dynamics of DCG4 has always been superior to the short-time performance of DCG2. This however need not be the case for the large-time limit. However, the performance of DCG2 is always better (short time) or equal (large time) to the performance of the Born-Markov secular approximation.

We have shown that DCG2 unconditionally preserves positivity. Going beyond [20], this also includes reservoirs that are not in equilibrium. In addition, the presentation in the interaction picture leads to a much simpler form of DCG2, such that now it appears at least as simple as (if not simpler than) the conventional Born-Markov theory. Positivity is not unconditionally preserved for higher orders of DCG.

Unfortunately, the DCG method is computationally quite demanding in the interesting case of large (continuous) reservoirs, as it requires the evaluation of high-dimensional integrals. As the dimension of some integrals can be reduced by analytical integration, the efficiency of DCG may therefore strongly depend on the structure of the bath correlation functions. For systems that are larger than the single spins considered here, it will also prove difficult to calculate the exponential of $\mathcal{L}^\tau t$ for all t and τ with moderate computational effort. If however the result is only of interest at a specific time (as is the case, for example, in adiabatic quantum computation), one only has to exponentiate a single matrix or—even more simply—evolve the density matrix according to a single Liouvillian. The fact that DCG2 unconditionally preserves positivity also for time-dependent system Hamiltonians renders the method a good candidate for analyzing the corrections of decoherence to adiabatic quantum computation [8] without the necessity of reverting to conventional Born-Markov secular theory [37].

ACKNOWLEDGMENTS

G.S. gratefully acknowledges discussions with J. Eisert, C. Emary, G. Kiesslich, R. Schützhold, and M. Vogl.

APPENDIX A: APPROXIMATE STEADY STATE OF THE SPIN-BOSON MODEL

Starting from Hamiltonian (34) we obtain with the abbreviations (we use bold symbols for operators in the Heisenberg picture)

$$\boldsymbol{s}_k = h_k \boldsymbol{b}_k + h_k^* \boldsymbol{b}_k^\dagger, \quad \boldsymbol{a}_k = i(h_k \boldsymbol{b}_k - h_k^* \boldsymbol{b}_k^\dagger) \tag{A1}$$

a set of equations for the time evolutions of $\langle \boldsymbol{\sigma}^x \rangle$, $\langle \boldsymbol{\sigma}^y \rangle$, $\langle \boldsymbol{\sigma}^z \rangle$, $\langle \boldsymbol{\sigma}^x \boldsymbol{s}_k \rangle$, $\langle \boldsymbol{\sigma}^x \boldsymbol{a}_k \rangle$, $\langle \boldsymbol{\sigma}^y \boldsymbol{s}_k \rangle$, $\langle \boldsymbol{\sigma}^y \boldsymbol{a}_k \rangle$, $\langle \boldsymbol{\sigma}^z \boldsymbol{s}_k \rangle$, and $\langle \boldsymbol{\sigma}^z \boldsymbol{a}_k \rangle$ in the Heisenberg picture, which is unfortunately not closed. However, we can achieve closure by assuming factorization of the expectation values and stationarity of the reservoir,

$$\left\langle \boldsymbol{\sigma}^{x/y/z} \sum_{k'} (\boldsymbol{s}_{k'} \boldsymbol{s}_k + \boldsymbol{s}_k \boldsymbol{s}_{k'}) \right\rangle = 2 \langle \boldsymbol{\sigma}^{x/y/z} \rangle \langle \boldsymbol{s}_k^2 \rangle,$$

$$\langle \boldsymbol{s}_k^2 \rangle = |h_k|^2 [1 + 2n(\omega_k)],$$

$$\left\langle \boldsymbol{\sigma}^{x/y/z} \sum_{k'} (\boldsymbol{s}_{k'} \boldsymbol{a}_k + \boldsymbol{a}_k \boldsymbol{s}_{k'}) \right\rangle = 0,$$

$$\left\langle \sum_{k'} (\boldsymbol{s}_{k'} \boldsymbol{a}_k - \boldsymbol{a}_k \boldsymbol{s}_{k'}) \right\rangle = -2i |h_k|^2, \tag{A2}$$

which is consistent with the Born approximation. We can then analyze the steady state of the resulting equations and obtain the same results as discussed before. That is, for pure dephasing ($A = \sigma^z$) we obtain $\langle \boldsymbol{\sigma}_\infty^x \rangle = \langle \boldsymbol{\sigma}_\infty^y \rangle = 0$ and $\langle \boldsymbol{\sigma}_\infty^z \rangle = \langle \sigma_0^z \rangle$ as discussed in Sec. III C 2. Similarly for the dissipative case ($A = \sigma^x$) we obtain $\langle \boldsymbol{\sigma}_\infty^x \rangle = \langle \boldsymbol{\sigma}_\infty^y \rangle = 0$ and $\langle \boldsymbol{\sigma}_\infty^z \rangle = \frac{1 - e^{-\beta \varepsilon_d}}{1 + e^{-\beta \varepsilon_d}}$, which is consistent with Eq. (51) in Sec. III C 3.

APPENDIX B: EXACT SOLUTION OF THE FANO-ANDERSON MODEL FOR LORENTZIAN TUNNELING RATES

From Hamiltonian (56) we can calculate the time evolution of the fermionic operators in the Heisenberg picture (we use bold operator symbols to denote the Heisenberg picture and exploit the anticommutation relations throughout),

$$\dot{\boldsymbol{d}} = -i\varepsilon_d \boldsymbol{d} + i\lambda \sum_k [t_{kL}^* \boldsymbol{c}_{k\mathbf{L}} + t_{kR}^* \boldsymbol{c}_{k\mathbf{R}}],$$

$$\dot{\boldsymbol{c}}_{k\mathbf{L}} = -i\omega_{kL} \boldsymbol{c}_{k\mathbf{L}} + i\lambda t_{kL} \boldsymbol{d},$$

$$\dot{\boldsymbol{c}}_{k\mathbf{R}} = -i\omega_{kR} \boldsymbol{c}_{k\mathbf{R}} + i\lambda t_{kR} \boldsymbol{d}, \tag{B1}$$

which already form a closed set of equations. These equations can be Laplace transformed [where $\boldsymbol{d}(t) \to \tilde{d}(z)$ and $\dot{\boldsymbol{d}}(t) \to -d + z\tilde{d}(z)$ and similarly for the other operators].

In Laplace space, we can eliminate $\tilde{c}_{kL}(z)$ and $\tilde{c}_{kR}(z)$ to solve the resulting equations for

$$\tilde{d}(z) = \frac{d + i\lambda\sum_k\left(\frac{t_{kL}^* c_{kL}}{z+i\omega_{kL}} + \frac{t_{kR}^* c_{kR}}{z+i\omega_{kR}}\right)}{z + i\varepsilon_d + \lambda^2\sum_k\left(\frac{|t_{kL}|^2}{z+i\omega_{kL}} + \frac{|t_{kR}|^2}{z+i\omega_{kR}}\right)} = \frac{d + i\lambda\sum_k\left(\frac{t_{kL}^* c_{kL}}{z+i\omega_{kL}} + \frac{t_{kR}^* c_{kR}}{z+i\omega_{kR}}\right)}{z + i\varepsilon_d + \frac{\lambda^2}{2\pi}\int_{-\infty}^{+\infty}\frac{\Gamma_L(\omega)+\Gamma_R(\omega)}{z+i\omega}d\omega}$$

$$= \frac{(z+\delta_L+i\varepsilon_L)(z+\delta_R+i\varepsilon_R)\left[d + i\lambda\sum_k\left(\frac{t_{kL}^* c_{kL}}{z+i\omega_{kL}} + \frac{t_{kR}^* c_{kR}}{z+i\omega_{kR}}\right)\right]}{(z+i\varepsilon_d)(z+\delta_L+i\varepsilon_L)(z+\delta_R+i\varepsilon_R) + \frac{\lambda^2}{2}[\Gamma_L^0\delta_L(z+\delta_R+i\varepsilon_R) + \Gamma_R^0\delta_R(z+\delta_L+i\varepsilon_L)]}, \tag{B2}$$

where in the last line we have already assumed Lorentzian tunneling rates (62). The inverse Laplace transform (Bromwick integral [38]) can be performed by the theorem of residues $\boldsymbol{d}(t) = \sum_i \text{Res}\, \tilde{d}(z)e^{+zt}|_{z=z_i}$, where z_i denote the poles of $\tilde{d}(z)$. Denoting the roots of

$$(z+i\varepsilon_d)(z+\delta_L+i\varepsilon_L)(z+\delta_R+i\varepsilon_R) + \frac{\lambda^2}{2}[\Gamma_L^0\delta_L(z+\delta_R+i\varepsilon_R) + \Gamma_R^0\delta_R(z+\delta_L+i\varepsilon_L)] = (z-z_1)(z-z_2)(z-z_3) \tag{B3}$$

by z_1, z_2, and z_3, respectively, we can easily calculate the residues. (In case of degenerate roots, one may either use residue formulas for higher-order poles or simply perform analytic continuation of the solution for first-order poles.) For $z_1 \neq z_2$, $z_1 \neq z_3$, and $z_2 \neq z_3$ we obtain the solution

$$\begin{aligned}
\boldsymbol{d}(t) = {} & \left[+\frac{(z_1+\delta_L+i\varepsilon_L)(z_1+\delta_R+i\varepsilon_R)e^{z_1 t}}{(z_1-z_2)(z_1-z_3)} + \frac{(z_2+\delta_L+i\varepsilon_L)(z_2+\delta_R+i\varepsilon_R)e^{z_2 t}}{(z_2-z_1)(z_2-z_3)} + \frac{(z_3+\delta_L+i\varepsilon_L)(z_3+\delta_R+i\varepsilon_R)e^{z_3 t}}{(z_3-z_1)(z_3-z_2)}\right]d \\
& + i\lambda\sum_k\left[+\frac{(z_1+\delta_L+i\varepsilon_L)(z_1+\delta_R+i\varepsilon_R)e^{z_1 t}}{(z_1-z_2)(z_1-z_3)(z_1+i\omega_{kL})} + \frac{(z_2+\delta_L+i\varepsilon_L)(z_2+\delta_R+i\varepsilon_R)e^{z_2 t}}{(z_2-z_1)(z_2-z_3)(z_2+i\omega_{kL})} + \frac{(z_3+\delta_L+i\varepsilon_L)(z_3+\delta_R+i\varepsilon_R)e^{z_3 t}}{(z_3-z_1)(z_3-z_2)(z_3+i\omega_{kL})}\right. \\
& \left.+\frac{(-i\omega_{kL}+\delta_L+i\varepsilon_L)(-i\omega_{kL}+\delta_R+i\varepsilon_R)e^{-i\omega_{kL}t}}{(-i\omega_{kL}-z_1)(-i\omega_{kL}-z_2)(-i\omega_{kL}-z_3)}\right]t_{kL}^* c_{kL} + i\lambda\sum_k\left[+\frac{(z_1+\delta_L+i\varepsilon_L)(z_1+\delta_R+i\varepsilon_R)e^{z_1 t}}{(z_1-z_2)(z_1-z_3)(z_1+i\omega_{kR})}\right. \\
& + \frac{(z_2+\delta_L+i\varepsilon_L)(z_2+\delta_R+i\varepsilon_R)e^{z_2 t}}{(z_2-z_1)(z_2-z_3)(z_2+i\omega_{kR})} + \frac{(z_3+\delta_L+i\varepsilon_L)(z_3+\delta_R+i\varepsilon_R)e^{z_3 t}}{(z_3-z_1)(z_3-z_2)(z_3+i\omega_{kR})} \\
& \left.+\frac{(-i\omega_{kR}+\delta_L+i\varepsilon_L)(-i\omega_{kR}+\delta_R+i\varepsilon_R)e^{-i\omega_{kR}t}}{(-i\omega_{kR}-z_1)(-i\omega_{kR}-z_2)(-i\omega_{kR}-z_3)}\right]t_{kR}^* c_{kR}.
\end{aligned} \tag{B4}$$

With taking the initial conditions as $\langle c_{k'L}^\dagger c_{kL}\rangle = \delta_{kk'} f_L(\omega_{kL})$ and $\langle c_{k'R}^\dagger c_{kR}\rangle = \delta_{kk'} f_R(\omega_{kR})$ and $\langle c_{k'R}^\dagger c_{kL}\rangle = 0$, we obtain for $n(t) = \langle \boldsymbol{d}^\dagger(t)\boldsymbol{d}(t)\rangle$ the expression

$$\begin{aligned}
n(t) = {} & \left|\frac{(z_1+\delta_L+i\varepsilon_L)(z_1+\delta_R+i\varepsilon_R)e^{z_1 t}}{(z_1-z_2)(z_1-z_3)} + \frac{(z_2+\delta_L+i\varepsilon_L)(z_2+\delta_R+i\varepsilon_R)e^{z_2 t}}{(z_2-z_1)(z_2-z_3)} + \frac{(z_3+\delta_L+i\varepsilon_L)(z_3+\delta_R+i\varepsilon_R)e^{z_3 t}}{(z_3-z_1)(z_3-z_2)}\right|^2 n_0 \\
& + \frac{\lambda^2}{2\pi}\int_{-\infty}^{+\infty}[\Gamma_L(\omega)f_L(\omega) + \Gamma_R(\omega)f_R(\omega)]\left|\frac{(z_1+\delta_L+i\varepsilon_L)(z_1+\delta_R+i\varepsilon_R)e^{z_1 t}}{(z_1-z_2)(z_1-z_3)(z_1+i\omega)} + \frac{(z_2+\delta_L+i\varepsilon_L)(z_2+\delta_R+i\varepsilon_R)e^{z_2 t}}{(z_2-z_1)(z_2-z_3)(z_2+i\omega)}\right. \\
& \left.+\frac{(z_3+\delta_L+i\varepsilon_L)(z_3+\delta_R+i\varepsilon_R)e^{z_3 t}}{(z_3-z_1)(z_3-z_2)(z_3+i\omega)} + \frac{(-i\omega+\delta_L+i\varepsilon_L)(-i\omega+\delta_R+i\varepsilon_R)e^{-i\omega t}}{(-i\omega-z_1)(-i\omega-z_2)(-i\omega-z_3)}\right|^2 d\omega.
\end{aligned} \tag{B5}$$

In the large-time limit, this considerably simplifies (using Re $z_i < 0$). Conventionally, λ^2 is absorbed in $\Gamma_L(\omega)$ and $\Gamma_R(\omega)$ and by setting $\lambda \to 1$ we explicitly recover the well-known steady-state results in the literature. [Compare, e.g., Eq. (12.27) of Ref. [34] with using Lorentzian tunneling rates of form (62) and Eqs. (12.30) and (12.31) of Ref. [34] with $n_\infty = \frac{-i}{2\pi}\int_{-\infty}^{+\infty} G^<(\omega)d\omega$].

---

[1] P. W. Shor, Quantum Inf. Process. **3**, 5 (2004).
[2] L. K. Grover, Phys. Rev. Lett. **79**, 325 (1997).
[3] M. A. Nielsen and I. L. Chuang, *Quantum Computation and Quantum Information* (Cambridge University Press, Cambridge, 2000).
[4] H.-P. Breuer and F. Petruccione, *The Theory of Open Quantum Systems* (Oxford University Press, Oxford, 2002).
[5] R. Raussendorf and H. J. Briegel, Phys. Rev. Lett. **86**, 5188 (2001).
[6] R. Raussendorf, D. E. Browne, and H. J. Briegel, Phys. Rev. A

68, 022312 (2003).
[7] J. Pachos and P. Zanardi, Int. J. Mod. Phys. B **15**, 1257 (2001).
[8] E. Farhi *et al.*, Science **292**, 472 (2001); E. Farhi, J. Goldstone, S. Gutmann, and M. Sipser, e-print arXiv:quant-ph/0001106.
[9] M. Schlosshauer, *Decoherence and the Quantum-to-Classical Transition* (Springer-Verlag, Berlin, 2007).
[10] Y. Zhao and G. H. Chen, Phys. Rev. E **65**, 056120 (2002).
[11] S. Stenholm and M. Jakob, J. Mod. Opt. **51**, 841 (2004).
[12] R. S. Whitney, J. Phys. A **41**, 175304 (2008).
[13] D. Taj and F. Rossi, Phys. Rev. A **78**, 052113 (2008).
[14] P. Pechukas, Phys. Rev. Lett. **73**, 1060 (1994); R. Alicki, *ibid.* **75**, 3020 (1995); P. Pechukas, *ibid.* **75**, 3021 (1995).
[15] D. P. DiVincenzo, Fortschr. Phys. **48**, 771 (2000).
[16] D. P. DiVincenzo and D. Loss, Phys. Rev. B **71**, 035318 (2005).
[17] S. Maniscalco, Phys. Rev. A **75**, 062103 (2007).
[18] P. Zedler, G. Schaller, G. Kießlich, C. Emary, and T. Brandes, e-print arXiv:0902.2118.
[19] U. Kleinekathöfer, J. Chem. Phys. **121**, 2505 (2004).
[20] G. Schaller and T. Brandes, Phys. Rev. A **78**, 022106 (2008).
[21] G. Lindblad, Commun. Math. Phys. **48**, 119 (1976).
[22] M. M. Wolf, J. Eisert, T. S. Cubitt, and J. I. Cirac, Phys. Rev. Lett. **101**, 150402 (2008).
[23] S. Liu and H. Neudecker, Statistical Papers **36**, 287 (1995).
[24] C. Emary, Phys. Rev. A **78**, 032105 (2008).
[25] R. S. Varga, *Gershgorin and His Circles* (Springer-Verlag, Berlin, 2004).
[26] H. Krovi, O. Oreshkov, M. Ryazanov, and D. A. Lidar, Phys. Rev. A **76**, 052117 (2007).
[27] U. Weiss, *Quantum Dissipative Systems* (World Scientific, Singapore, 1993).
[28] T. Brandes, Phys. Rep. **408**, 315 (2005).
[29] W. G. Unruh, Phys. Rev. A **51**, 992 (1995).
[30] D. A. Lidar, Z. Bihary, and K. B. Whaley, Chem. Phys. **268**, 35 (2001).
[31] A. J. Leggett *et al.*, Rev. Mod. Phys. **59**, 1 (1987).
[32] U. Fano, Phys. Rev. **124**, 1866 (1961).
[33] P. W. Anderson, Phys. Rev. **124**, 41 (1961).
[34] H. Haug and A.-P. Jauho, *Quantum Kinetics in Transport and Optics of Semiconductors* (Springer, Berlin, 2008).
[35] G. Stefanucci and C.-O. Almbladh, Phys. Rev. B **69**, 195318 (2004).
[36] B. Elattari and S. A. Gurvitz, Phys. Rev. A **62**, 032102 (2000).
[37] A. M. Childs, E. Farhi, and J. Preskill, Phys. Rev. A **65**, 012322 (2001).
[38] G. B. Arfken and H. J. Weber, *Mathematical Methods for Physicists* (Elsevier, Oxford, 2005).